eLife

Reviewed Preprint
v2 • January 31, 2025
Revised by authors

Reviewed Preprint
v1 • August 22, 2024

Developmental Biology

# Impaired yolk sac NAD metabolism disrupts murine embryogenesis with relevance to human birth defects

**Kayleigh Bozon, Hartmut Cuny, Delicia Z Sheng, Ella MMA Martin, Alena Sipka, Paul Young, David T Humphreys, Sally L Dunwoodie**

Victor Chang Cardiac Research Institute, Sydney, Australia • School of Clinical Medicine, Faculty of Medicine and Health, University of New South Wales, Sydney, Australia



**eLife Assessment**

NAD deficiency perturbs embryonic development resulting in multiple congenital malformations, collectively termed Congenital NAD Deficiency Disorder (CNDD). The authors report **fundamental** findings demonstrating that extra-embryonic visceral yolk sac endoderm is critical for NAD de novo synthesis during early organogenesis and perturbations of this pathway may underlie CNDD. The authors combine gene expression with metabolic assays to provide **solid** evidence of an essential role of the extra-embryonic visceral yolk sac in both mouse and human embryos.

https://doi.org/10.7554/eLife.97649.2.sa3

## Abstract

Congenital malformations can originate from numerous genetic or non-genetic factors but in most cases the causes are unknown. Genetic disruption of nicotinamide adenine dinucleotide (NAD) *de novo* synthesis causes multiple malformations, collectively termed Congenital NAD Deficiency Disorder (CNDD), highlighting the necessity of this pathway during embryogenesis. Previous work in mice shows that NAD deficiency perturbs embryonic development specifically when organs are forming. While the pathway is predominantly active in the liver postnatally, the site of activity prior to and during organogenesis is unknown.

Here, we used a mouse model of human CNDD and assessed pathway functionality in embryonic livers and extraembryonic tissues via gene expression, enzyme activity and metabolic analyses. We found that the extra-embryonic visceral yolk sac endoderm exclusively synthesises NAD *de novo* during early organogenesis before the embryonic liver takes over this function. Under CNDD-inducing conditions, visceral yolk sacs had reduced NAD levels and altered NAD-related metabolic profiles, affecting embryo metabolism. Expression of requisite pathway genes is conserved in the equivalent yolk sac cell type in humans.

Our findings show that visceral yolk sac-mediated NAD *de novo* synthesis activity is essential for mouse embryogenesis and its perturbation causes CNDD. As mouse and human yolk sacs

are functionally homologous, our data improve the understanding of human congenital malformation causation.

## Introduction

Congenital malformations with substantial medical consequences are a major health burden because of their severity and high prevalence, occurring in approximately 3% of live births (Moorthie et al., 2018). Causes of congenital malformation are complex and diverse and can involve genetic as well as environmental factors, complicating the identification of aetiologies. Consequently, the underlying causes of malformation are still unknown in the majority of cases.

Disruption of the nicotinamide adenine dinucleotide (NAD) *de novo* Synthesis Pathway, by which L-tryptophan is converted to NAD (**Figure 1A**), causes congenital malformations of varying types and severity. It affects organs and structures such as heart, kidney, vertebrae and others, and is termed Congenital NAD Deficiency Disorder (CNDD) (Dunwoodie et al., 2023). NAD, referring to its oxidised and reduced form (NAD+ and NADH), is both a critical redox cofactor present in all living cells and an essential co-enzyme involved in a diverse range of cellular functions. Besides NAD *de novo* synthesis from L-tryptophan, mammals also generate NAD from vitamin B3, a collective term for the vitamers nicotinic acid (NA), nicotinamide (NAM), nicotinamide mononucleotide (NMN), and nicotinamide riboside (NR), via the Preiss-Handler and NAD Salvage Pathways (**Figure 1A**).

In all CNDD cases identified to date, affected patients had biallelic pathogenic variants in either *KYNU* (kynureninase), *HAAO* (3-hydroxyanthranilic acid 3,4-dioxygenase) or *NADSYN1* (NAD synthetase 1), all essential genes of NAD *de novo* synthesis (Dunwoodie et al., 2023; Shi et al., 2017; Szot et al., 2020; Szot et al., 2024). *Kynu*, *Haao*, or *Nadsyn1* homozygous-null mouse models in combination with diets low in vitamin B3 recapitulated the human phenotypes (Shi et al., 2017; Szot et al., 2024). When maternal vitamin B3 provision was restricted during pregnancy, it induced CNDD-like defects specifically in homozygous-null mouse embryos, and these embryos had no malformations when the mother was provided sufficient dietary vitamin B3 to bypass their genetic block, as here NAD is synthesised via the Preiss-Handler Pathway or NAD Salvage Pathway (**Figure 1A**) (Shi et al., 2017). Conversely, embryos of wild-type mothers given diets low in L-tryptophan and depleted in vitamin B3 exhibit NAD deficiency and CNDD-like malformations, with phenotypic severity exacerbated by gene-environment interactions via *Haao* or *Nadsyn1* heterozygosity (Cuny et al., 2020; Szot et al., 2024).

These CNDD mouse models suggest that NAD *de novo* synthesis is active in the conceptus and is required for normal organ development unless sufficient vitamin B3 is supplied by the mother. In adult mice, NAD *de novo* synthesis occurs in the liver and to a very minor extent in the kidney (Liu et al., 2018; Wang et al., 2023). But mouse embryos are susceptible to CNDD between embryonic day (E) 7.5 and E12.5, before the embryo has developed a functional liver. Therefore, NAD *de novo* synthesis is likely active in another tissue during this time window of susceptibility.

The major components of the mammalian conceptus are the embryo itself and two extraembryonic organs, the chorioallantoic placenta and the visceral yolk sac (hereon yolk sac). Perturbation of either extraembryonic organ function can induce malformations in the embryo (Brent & Fawcett, 1998; Brent et al., 1971; Perez-Garcia et al., 2018). Therefore, to determine where NAD *de novo* synthesis activity occurs in the conceptus, we assessed pathway function in these extraembryonic tissues during the CNDD-susceptible organogenesis stages, and in the embryonic liver once formed. We quantified expression of NAD *de novo* Synthesis Pathway genes, HAAO enzyme activity, and metabolites formed during the synthesis and consumption of NAD. We

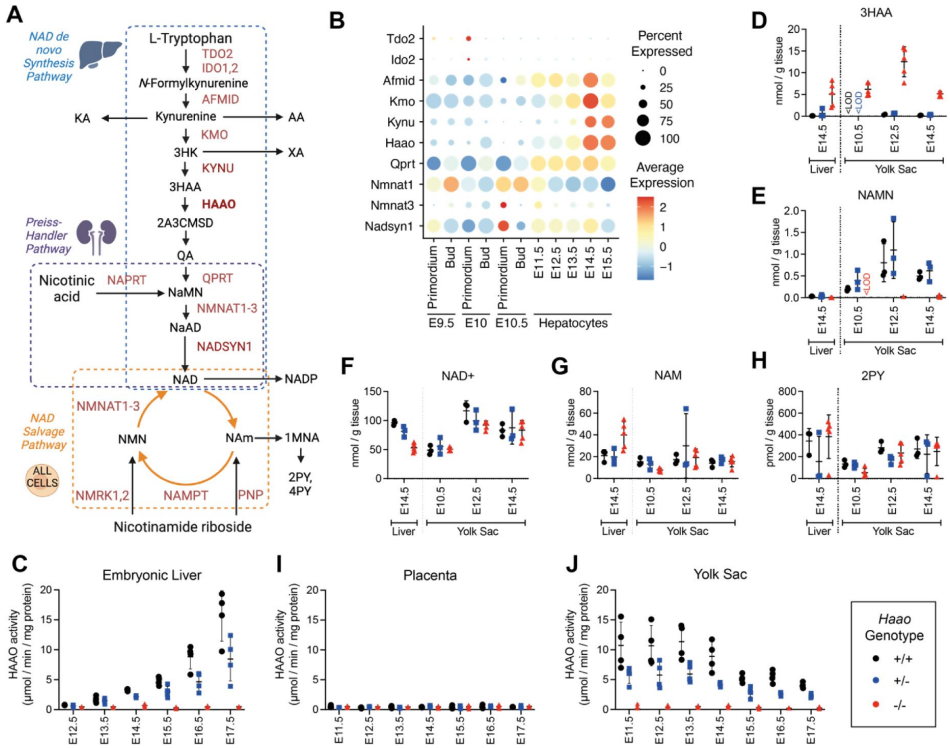


## Figure 1

### NAD *de novo* synthesis is performed by the yolk sac during organogenesis and later by the embryonic liver.

(A) Schematic overview of the NAD synthesis pathways. The NAD *de novo* Synthesis Pathway (blue box) converts the essential amino acid L-tryptophan to NAD and is predominantly performed by the liver (Liu et al., 2018). The Preiss-Handler Pathway (purple box) converts nicotinic acid to NAD in the kidney. The Salvage Pathway (orange box), performed in all cells, salvages the product of NAD consuming enzymes, nicotinamide (NAM), back to NAD. When NAD levels are in excess, NAM is converted to 1-methylnicotinamide (1MNA), N-methyl-2-pyridone-5-carboxamide (2PY) and N-methyl-4-pyridone-5-carboxamide (4PY) and excreted. Enzymes are in red, metabolites in black. (B) Re-analysis of published scRNA-seq data (Mu et al., 2020) via DotPlot showing average log normalised expression (heatmap colour) and proportion of cells (circle size) of requisite NAD *de novo* Synthesis Pathway Genes in the hepatocyte lineage between embryonic day (E) 9.5 and E15.5. (C) HAAO enzyme activity in embryonic liver from E12.5 to E17.5. (D-H) Concentration of core NAD *de novo* Synthesis Pathway metabolites in the embryonic liver (E14.5) and yolk sac (E10.5-14.5). Metabolite concentrations are normalised to wet weight measured at dissection. (I,J) HAAO enzyme activity in placenta (I) and visceral yolk sac (J) samples collected between E11.5 to E17.5. *Haao*$^{+/+}$ (black circle), *Haao*$^{+/-}$ (blue square) and *Haao*$^{-/-}$ (red triangle). Bars indicate the mean ± standard deviation. See **Table S1** for HAAO activity numerical values and Tables S2 and S3 for metabolite concentration values, including those of additional NAD-related metabolites. 3HK = 3-hydroxykynurenine, 3HAA = 3-hydroxyanthranilic acid, NAMN = nicotinic acid mononucleotide, KA = kynurenic acid, AA = anthranilic acid, XA = xanthurenic acid, QA = quinolinic acid, NaMN = nicotinic acid mononucleotide, NaAD = nicotinic acid adenine dinucleotide, NADP = nicotinamide adenine dinucleotide phosphate, NMN = nicotinamide mononucleotide, <LOD = below the limit of detection.

identified yolk sac endoderm cells as the site of NAD *de novo* synthesis during organogenesis in mice. A comparison of mouse and human single-cell RNA datasets indicates that these findings in mouse are relevant to humans.

# Results

## NAD *de novo* synthesis in the embryonic liver is active after organogenesis in mice

NAD is synthesised *de novo* from L-tryptophan, predominantly in the liver. In addition, all cells salvage NAD from NAM in the circulation, with circulatory NAM levels dependent on NAD *de novo* synthesis in the liver (Liu et al., 2018). We have shown in mice that the conceptus is able to synthesise NAD *de novo* prior to E12.5 (Shi et al., 2017); however, it is unclear if or when the embryonic liver is capable of NAD *de novo* synthesis. In mice, liver primordial cells are present around E9.5 to E10.5, hepatocytes are present from E11.5, and enzymes of the pathway are detected from E13.5 (Burke et al., 2018; Mu et al., 2020; Notenboom et al., 1997; Yang et al., 2017).

To determine when NAD *de novo* Synthesis Pathway activity commences in hepatocytes during embryogenesis, we re-analysed published murine single-cell RNA-seq (scRNA-seq) data for the hepatic lineage (liver primordium, liver bud, and hepatocytes) (Mu et al., 2020) (**Figure 1B**). *Tdo2* and *Ido2*, encoding tryptophan-catabolising enzymes, were negligibly expressed at all stages. Expression of subsequent pathway genes *Afmid*, *Kmo*, *Haao*, *Qprt* and *Nadsyn1*, required for NAD *de novo* synthesis from kynurenine (also referred to as the kynurenine pathway), progressively increased during embryogenesis (**Figure 1B**, **Figure S1**), though the time of onset and proportion of cells varied between genes. Nonetheless, all were expressed by E14.5 (**Figure 1B**). HAAO enzyme assays were performed on $Haao^{+/+}$, $Haao^{+/-}$and $Haao^{-/-}$ embryonic livers, isolated from mothers provided a diet rich in L-tryptophan and vitamin B3 (Breeder diet, see Methods). The livers showed limited HAAO activity at E12.5 and a gradually increase at subsequent developmental stages. Furthermore, HAAO activity correlated with the number of functional *Haao* alleles and was significantly different between genotypes at all stages assessed (**Figure 1C**, **Table S1**). Whole E11.5 embryos as well as E14.5 embryos with their livers removed had negligible HAAO enzymatic activity (**Figure S2**, **Table S1**), confirming that no other embryonic tissue apart from the liver is capable of NAD *de novo* synthesis.

To validate that the pathway is functional at E14.5 in the liver, we quantified NAD+ and 11 NAD-related metabolites in $Haao^{+/+}$, $Haao^{+/-}$ and $Haao^{-/-}$ liver samples using ultra-high-performance liquid chromatography– tandem mass spectrometry (UHPLC-MS/MS) (Cuny et al., 2021) (**Table S2**). Differential accumulation of metabolites upstream and downstream of the *Haao* genetic block is a defining characteristic of enzyme loss-of-function in both mice and humans (Shi et al., 2017; Szot et al., 2024). Accordingly, $Haao^{-/-}$ E14.5 livers had significantly elevated levels of the upstream metabolite 3HAA (18-fold) relative to $Haao^{+/+}$, whereas the downstream metabolites QA and NAMN were undetectable and significantly decreased (4-fold), respectively (**Figure 1D,E**, **Table S2**,). NAD+ levels were also significantly affected by the loss of functional *Haao* alleles (**Figure 1F**, **Table S2**), with the lowest concentration measured in $Haao^{-/-}$ embryonic livers. By contrast, levels of the NAD Salvage Pathway metabolite NAM were 2-fold higher in $Haao^{-/-}$, compared to $Haao^{+/+}$ and $Haao^{+/-}$ livers (**Figure 1G**, **Table S2**) and levels of the waste products $N^1$-methyl-2-pyridone-5-carboxamide (2PY) and $N^1$-methyl-4-pyridone-3-carboxamide (4PY) were similar between *Haao* genotypes (**Figure 1H**, **Table S2**).This suggests that NAD Salvage Pathway activity compensated for the loss of NAD *de novo* synthesis activity in $Haao^{-/-}$ embryos.

Together, these data confirm that NAD *de novo* Synthesis Pathway gene expression occurs in the developing liver from E12.5 onwards and the pathway is functional by E14.5, which is in line with expression of genes encoding other metabolic enzymes (Mu et al., 2020). However, as CNDD malformations occur in *Haao*$^{-/-}$ mouse embryos when NAD is deficient between E7.5 and E12.5 (Shi et al., 2017), NAD *de novo* synthesis must occur elsewhere in the earlier-stage conceptus.

## NAD *de novo* synthesis occurs during early organogenesis in the mouse yolk sac but not the placenta

In mammals, two likely candidate sites for extrahepatic NAD *de novo* synthesis are the chorioallantoic placenta and the yolk sac. First, we re-analysed published mouse E9.5-14.5 placenta scRNAseq data (Marsh & Blelloch, 2020) and found that NAD *de novo* Synthesis Pathway gene expression was scattered between the maternal decidual stroma *(Tdo2, Ido1, Ido2)* or various immune cell populations *(Afmid, Kmo, Kynu, Haao, Qprt, Nadsyn1)* but not in the conceptus-derived trophoblasts that constitute the bulk of placental tissue (**Figure S3**). Additionally, we showed that HAAO enzyme activity was absent in the mouse placenta between E11.5 and E17.5 (**Figure 1I**, **Table S1**). Combined, these data indicate that the murine placenta does not conduct NAD *de novo* synthesis.

Next, we quantified HAAO enzyme activity in the yolk sac between E11.5 and E17.5. By contrast to the placenta, *Haao*$^{+/+}$ and *Haao*$^{+/-}$ yolk sacs exhibited HAAO enzyme activity during early organogenesis (E11.5 to E13.5), after which it progressively declined (**Figure 1J**, **Table S1**). The decline in HAAO activity in the yolk sac coincided with its rise in the embryonic liver (**Figure 1C**, **Table S1**). In the absence of available stage-appropriate RNA-seq datasets for the yolk sac, we assessed NAD *de novo* Synthesis Pathway gene expression by RT-qPCR between E10.5 and E17.5. Transcript levels for early pathway genes (*Tdo2, Ido2, Afmid*) were similar across all stages, whereas expression of subsequent genes (*Kmo, Kynu, Haao, Qprt, Nadsyn1*) was highest at E10.5, then declined 2-10 fold by E17.5 (**Figure 2A,B**).

We quantified NAD+ and 10 NAD-related metabolites in *Haao*$^{+/+}$, *Haao*$^{+/-}$ and *Haao*$^{-/-}$ yolk sac samples at E10.5, E12.5, and E14.5. Metabolites spanning the entire NAD *de novo* Synthesis Pathway were quantifiable at all stages (**Table S3**). The yolk sac metabolite data were compared to the E14.5 embryonic liver by principal component analysis, which showed gestational age and *Haao*$^{-/-}$ genotype as the main determinants of variance in the NAD metabolism (**Figure 2C**). Metabolite levels, normalised to tissue weight, were generally low in E10.5 yolk sacs, similar to levels of E14.5 embryonic liver, and generally higher in E12.5 and E14.5 yolk sacs (**Figure 2D**, **Table S3**). *Haao*$^{-/-}$ yolk sacs also exhibited the metabolic signature characteristic of HAAO genetic block, with significant accumulation (~20-fold) of upstream 3HAA, and absence of the downstream NAMN relative to *Haao*$^{+/+}$ and *Haao*$^{+/-}$ yolk sacs at all stages (**Figure 1D,E**, **Table S3**). Downstream of NAMN, NAD+ levels were not significantly affected by *Haao* genotype at any stage (**Figure 1F**, **Table S3**). However, levels of the NAD Salvage Pathway metabolite NAM and waste metabolites 2PY and 4PY were significantly reduced in E10.5 *Haao*$^{-/-}$ yolk sacs relative to *Haao*$^{+/+}$ and *Haao*$^{+/-}$ (**Figure 1G,H**, **Table S3**), suggesting that loss of NAD *de novo* synthesis resulted in a metabolic adjustment of the NAD Salvage Pathway to maintain NAD levels.

These data, combined with the presence of HAAO activity and expression of all requisite pathway genes, confirmed that the yolk sac performs NAD *de novo* synthesis from at least E10.5 onwards and therefore is the site of NAD *de novo* Synthesis Pathway activity in the conceptus during organogenesis prior to the formation of a functional liver.

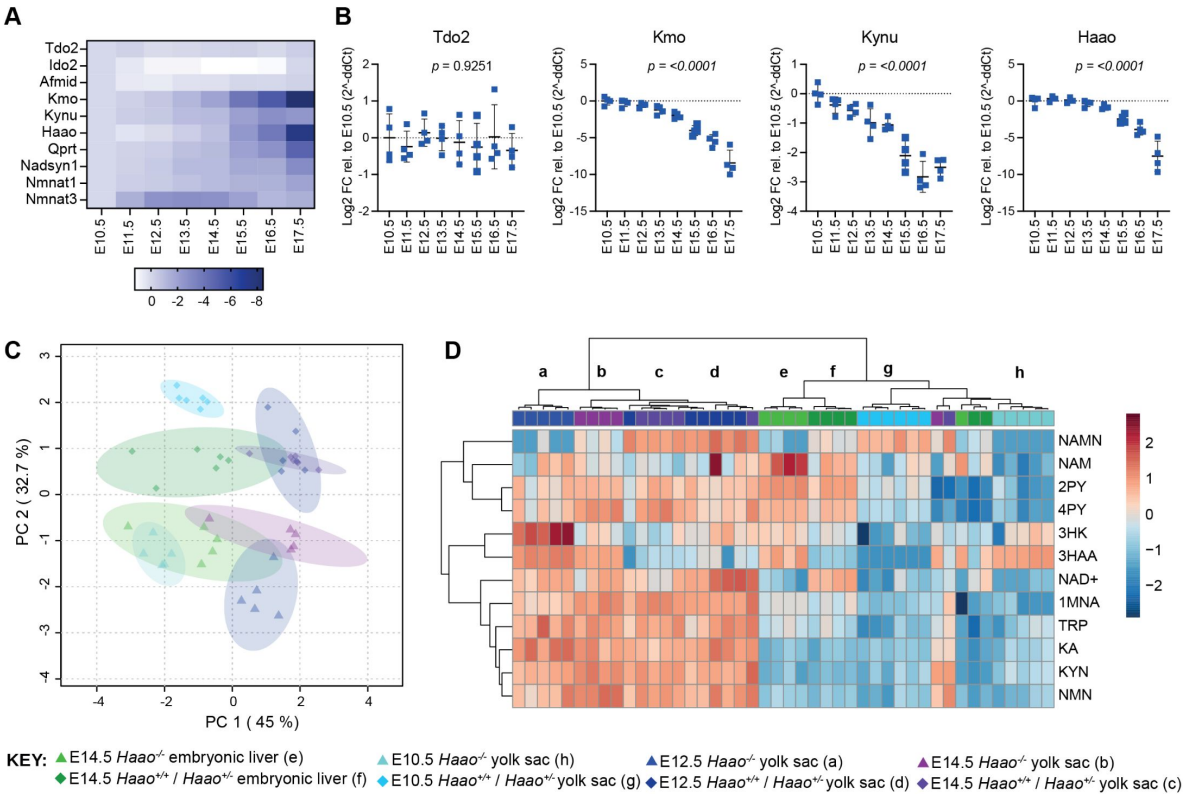


## Figure 2.

### The yolk sac performs NAD *de novo* synthesis from E10.5 onwards.

(A-B) Heatmap (A) and bar graphs (B) showing changes in core NAD *de novo* NAD Synthesis Pathway gene expression in *Haao*$^{+/-}$ visceral yolk sacs between E10.5 and E17.5 quantified by RT-qPCR (n = 4). Expression is calculated as log2 fold-changes relative to gene expression at E10.5 and normalised to two housekeeping genes, *Ubc* and *Ywhaz*. Bars indicate the mean ± standard deviation. Statistical significance was determined by one-way ANOVA. (C-D) NAD-related metabolite concentrations in visceral yolk sacs at embryonic day (E) 10.5, E12.5 and E14.5 were compared to metabolite concentrations in E14.5 embryonic livers. (C) Principal component analysis (PCA) of the concentrations of NAD and 11 related metabolites in the three tissues at each embryonic stage. Embryonic liver (green) and yolk sac (light blue, indigo, purple); triangles: *Haao*$^{-/-}$ tissues, diamonds: *Haao*$^{+/+}$ and *Haao*$^{+/-}$ tissues. The primary determinants of variance in the NAD metabolome were gestational age (PC 1) and *Haao* genotype (PC 2). (D) Heatmap showing wet weight normalised, log10 transformed, and Pareto scaled concentration of each quantified metabolite across all samples, tissues and timepoints. Clusters are labeled with lowercase letters corresponding to tissues and genotypes specified in the key. Consistent with the PCA, the metabolite profile of E10.5 yolk sacs clustered to that of E14.5 embryonic liver. Hierarchical clustering was performed using Euclidean as distance measure and Ward as a clustering method. See Tables S2 and S3 for numerical metabolite concentration values.

## NAD deficiency between E7.5 and E10.5 induces CNDD-related congenital anomalies in mice

Having confirmed that NAD *de novo* synthesis is performed in the yolk sac during early organogenesis, we next sought to understand how its activity is perturbed under conditions that cause CNDD. The data outlined above was generated using a diet rich in vitamin B3 which allows pregnant mice with a genetic block in the NAD *de novo* Synthesis Pathway to generate NAD via the Preiss-Handler and NAD Salvage Pathway and provide sufficient NAD precursors to their embryos for normal development. Due to higher metabolic rate and food intake per body weight in mice compared to humans (Bachmanov et al., 2002; Holliday et al., 1967), to induce CNDD in mice, pregnant females need to be given L-tryptophan and/or vitamin B3 restricted diets, thereby limiting their ability to provide NAD precursors to the embryos (Cuny et al., 2020; Shi et al., 2017; Szot et al., 2024). Given that NAD *de novo* synthesis is established in the yolk sac by E10.5, we placed *Haao*$^{-/-}$mothers on a NAD precursor-restricted diet specifically between E7.5 and E10.5. During this time window, L-tryptophan and vitamin B3 were removed from the chow and 1000 mg/L L-tryptophan and 3.5 mg/L nicotinic acid were supplemented in the drinking water (hereon referred to as NW3.5) (**Figure 3A**). Unlike wild-type and *Haao*$^{+/-}$ mice, *Haao*$^{-/-}$ mice can only use the vitamin B3 but not L-tryptophan in the diet to synthesise NAD. Here, *Haao*$^{-/-}$ females were mated with *Haao*$^{+/-}$ males and generated embryos with *Haao*$^{+/-}$and *Haao*$^{-/-}$ genotypes, of which only the former can use any L-tryptophan provided by the maternal circulation.

Embryos from mothers on the NW3.5 diet were assessed for the presence of congenital anomalies at E18.5. *Haao*$^{-/-}$ embryos were significantly smaller than their *Haao*$^{+/-}$ littermates (**Figure 3B**). Furthermore, 86.7% of *Haao*$^{-/-}$ embryos were malformed, with 83.3% (25/30) of them presenting with multiple defects (**Figure 3C**, **Table S4**). We identified malformations in organs and tissues previously associated with CNDD (Cuny et al., 2020; Shi et al., 2017). Kidney defects (in 83.3% of *Haao*$^{-/-}$ embryos) included hypoplasia or agenesis, as well a cyst observed in one kidney. In addition, shortened tails (73.3%), various structural heart defects (27.7%), digit and limb anomalies (40%), and vertebrae and rib defects (63.3%) including rib underdevelopment, sternum defects, vertebral fusions, butterfly vertebrae, and hemivertebrae were found (**Table S4**). By contrast, the ability to perform NAD de *novo* synthesis prevented NAD deficiency in *Haao*$^{+/-}$ littermate embryos; the only defect was a solitary case of heart ventricular septum defect (**Figure 3C**, **Table S4**).

These observations align with previous CNDD studies utilising *Haao*$^{-/-}$ mothers on a vitamin B3-restricted diet (Cuny et al., 2020; Shi et al., 2017). In addition, they show that restricting dietary precursor supply for three days only, between E7.5 and E10.5, is sufficient to cause CNDD malformation. This narrow window of susceptibility highlights the necessity of NAD *de novo* Synthesis Pathway activity in the yolk sac for normal development.

## The yolk sac has reduced NAD availability under conditions that induce congenital malformations

Having established the importance of E10.5 as a key stage of NAD *de novo* synthesis, we next characterised how maternal dietary NAD precursor-restriction between E7.5 and E10.5 affected levels of NAD and related metabolites in the yolk sac at E10.5. We previously showed that supplementing 15 mg/L nicotinic acid in the drinking water is sufficient to support normal development of *Haao*$^{-/-}$embryos (Shi et al., 2017). Therefore, yolk sac samples from the maternal NW15 dietary condition (**Figure 3A**) were collected as appropriate controls for comparison to NW3.5 samples.

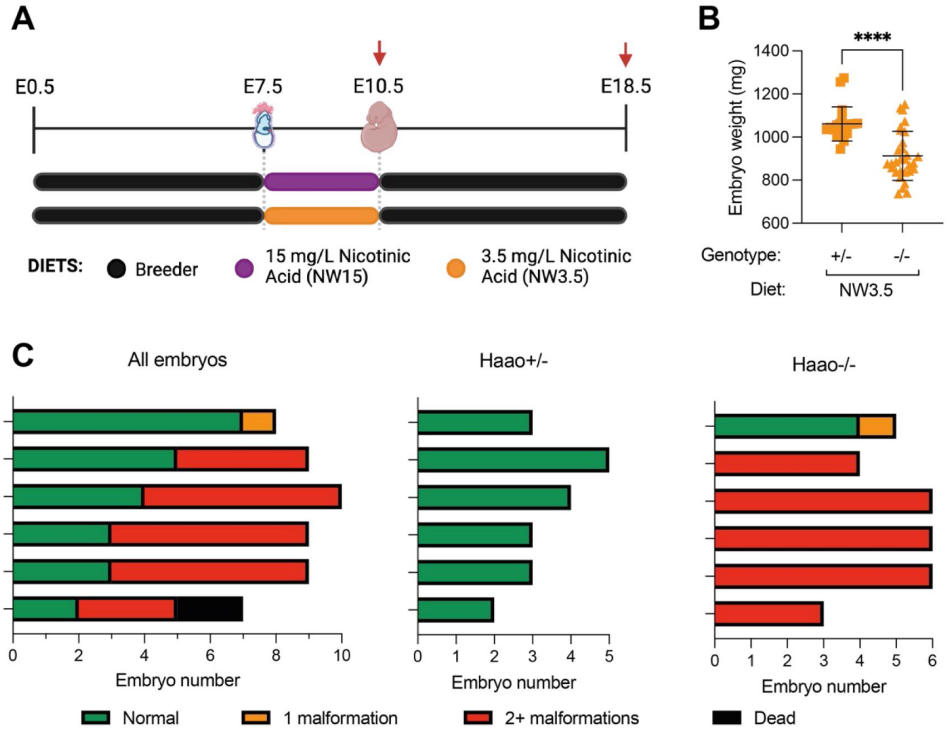


**Figure 3.**

**Congenital NAD Deficiency Disorder (CNDD) phenotypes and NAD deficiency can be induced in *Haao*$^{-/-}$ embryos by restricting maternal NAD precursor supply for three days.**

(A) Schematic overview of the dietary treatment to induce NAD deficiency and embryo malformations. Pregnant mice were provided Breeder diet, rich in L-tryptophan and vitamin B3, throughout gestation except for a three-day window between embryonic day (E) 7.5 and E10.5 during which feed lacking any NAD-precursor and drinking water supplemented with 1 g/L L-tryptophan and either 15 mg/L (NW15) or 3.5 mg/L (NW3.5) nicotinic acid was given. Red arrows indicate tissue collection timepoints. (B) Weights of *Haao*$^{+/-}$ (square) or *Haao*$^{-/-}$ (triangle) embryos at embryonic day (E) 18.5 collected from mothers on NW3.5 diet. Weights represent wet weight measured at dissection. Statistical significance was determined by Student's t-test with **** $p<0.0001$. Bars indicate the mean ± standard deviation. (C) Summary of the phenotypic outcomes of E18.5 embryos generated from the NW3.5 diet condition. Each bar represents a litter, with the graph on the left summarising data of entire litters and the other two separating the *Haao*$^{+/-}$ and *Haao*$^{-/-}$ embryos of each litter. Colours indicate the number of different congenital malformations observed in each embryo. Dead embryos (black) represented early resorptions and could not be genotyped.

Due to their small size, 2-3 yolk sacs were pooled per sample for NAD metabolite quantification by UHPLC-MS/MS. The diet itself had profound effects on the yolk sac metabolites (**Table S5**-**6**). Although L-tryptophan concentration in the drinking water was equivalent in both diets, its levels were lower in NW3.5 yolk sacs than NW15 (**Table S5**-**6**, **Figure 4A**). The abundance of NAD *de novo* synthesis pathway metabolites both upstream (3HAA) and downstream (QA, NAMN, NAAD) of the *Haao* genetic block was significantly altered in *Haao*$^{-/-}$ and *Haao*$^{+/-}$ yolk sacs, respectively, relative to their NW15 counterparts (**Figure 4B-E**,**Table S5**-**6**). Despite this, NAD+ levels were comparable between *Haao*$^{+/-}$ yolk sacs on both diets (**Figure 4F**, **Table S5**-**6**). By contrast, the inability of *Haao*$^{-/-}$ yolk sacs to perform NAD *de novo* synthesis resulted in a significant decline in NAD+ (54-71%) and NAM (69-77%) levels relative to *Haao*$^{+/-}$ on the equivalent diet (**Figure 4F-G**, **Table S5**-**6**). Yet, yolk sac NAD+ levels were lowest when the genetic disruption and dietary restriction were combined (NW3.5 *Haao*$^{-/-}$), confirming the importance of maternal provision in maintaining NAD+ levels when the yolk sac cannot generate NAD *de novo*.

## The NAD metabolome of the yolk sac and embryo correlate during early organogenesis

The yolk sac has a nutritional role in mammals as it uptakes and processes maternally derived macro-and micronutrients and transfers these to the embryo via their interconnected and expanding vasculature (Burton et al., 2016; Ornoy & Miller, 2023). In mice, histotrophic nutrition via the yolk sac is solely responsible for supporting the nutritional requirements of the developing embryo until the gradual transition to haemotrophic nutrition across the chorioallantoic placenta between E10 and 12 (Elmore et al., 2022). Therefore, we explored the effects of impaired NAD *de novo* synthesis of the yolk sac on NAD metabolite levels of the embryo.

We analysed the embryos that corresponded to the metabolically analysed yolk sacs above. Whilst we had to pool 2-3 yolk sacs at E10.5 for analysis, embryos were sufficiently large to be analysed individually with the embryo corresponding to one of the pooled yolk sacs. Contrary to observations at E18.5 (**Figure 3B**), *Haao* genotype had no effect on embryo weight within the same dietary condition, but embryos were significantly smaller on NW3.5 than NW15 (**Figure 4H**).Consistent with the yolk sac samples, the diet had a marked effect on embryonic NAD status, with NAD+ and the waste metabolites 2PY and 4PY significantly reduced in NW3.5 embryos relative to the same *Haao* genotype on the NW15 diet (**Figure 5E**,**G**,**H**, **Table S5**). However, in agreement with phenotypic outcome at E18.5, NAD+ levels of NW3.5 *Haao*$^{-/-}$embryos were significantly lower than those of *Haao*$^{+/-}$ embryos on the same diet (**Figure 5E**, **Table S5**).

NAD *de novo* Synthesis Pathway metabolites were quantifiable in embryos (**Figure 5A-D**, **Table S5**-**6**), with differential abundance of metabolite upstream and downstream of the *Haao* genetic block mirroring those observed in the yolk sac. Neither the placenta nor the embryonic liver synthesise NAD *de novo* at E10.5, suggesting that these metabolites either originate from the yolk sac, which is consistent with the connection of vitelline and embryonic vasculature, or that another embryonic cell type is synthesising NAD *de novo* at E10.5.

To test the latter option, we examined pathway gene expression in the embryo at E10.5 using the 'mouse organogenesis cell atlas' (MOCA) (Cao et al., 2019). Except for some limited *Afmid* and *Kynu* expression predominantly in immune cell populations, the requisite genes were not expressed, including in hepatocytes (**Figure S4**). Therefore, intermediary metabolites were seemingly exchanged between the yolk sac and the embryo. To explore this, we calculated the Pearson correlation for all measured NAD-related metabolites between corresponding yolk sacs and embryos. Protein-normalised concentrations of those metabolites differentially abundant by

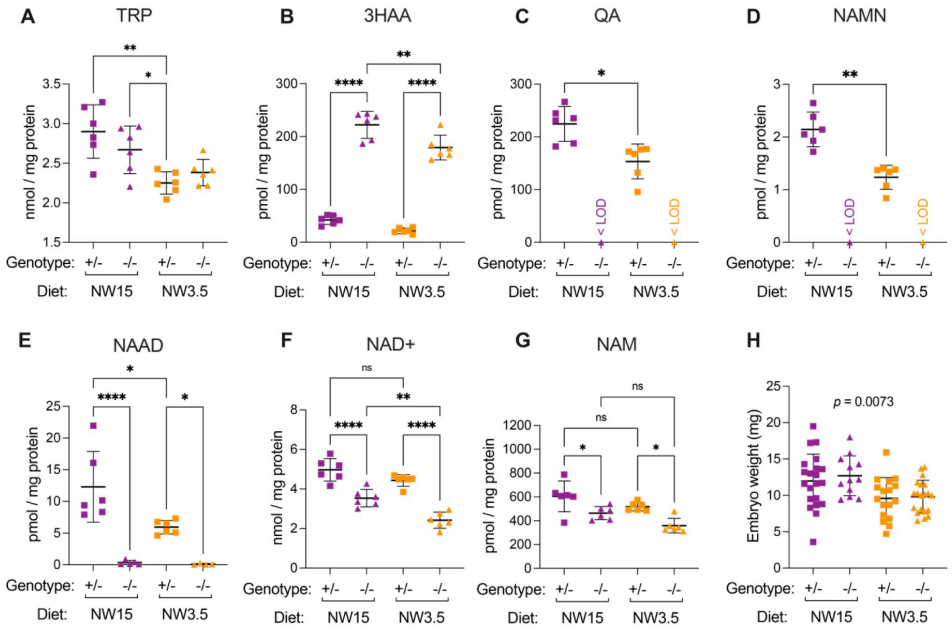


## Figure 4.

### The yolk sac NAD metabolome is affected by maternal dietary limitation of NAD precursors that causes embryo malformations.

(A-G) Concentration of NAD-related metabolites in E10.5 yolk sacs normalised to total protein content. (A) L-tryptophan (TRP), (B) 3-hydroxyanthranilic acid (3HAA), (C) quinolinic acid (QA), (D) nicotinic acid mononucleotide (NAMN), (E) nicotinic acid adenine dinucleotide (NAAD), (F) NAD+, (G) nicotinamide (NAM). (H) Wet weight of E10.5 embryos from the NW15 (purple) and NW3.5 (orange) diet conditions, measured at dissection. Bars indicate the mean ± standard deviation. The *Haao* genotype and diet are indicated below each graph. Statistical significance in (A-G) was calculated by one-way ANOVA with Tukey's multiple comparisons test with ns = not significant, * $p<0.05$, ** $p<0.01$, and **** $p<0.0001$. Statistical significance in (H) was calculated by one-way ANOVA with the $p$ value indicated above graph. <LOD = below the limit of detection. For numerical values, see **Table S5**.

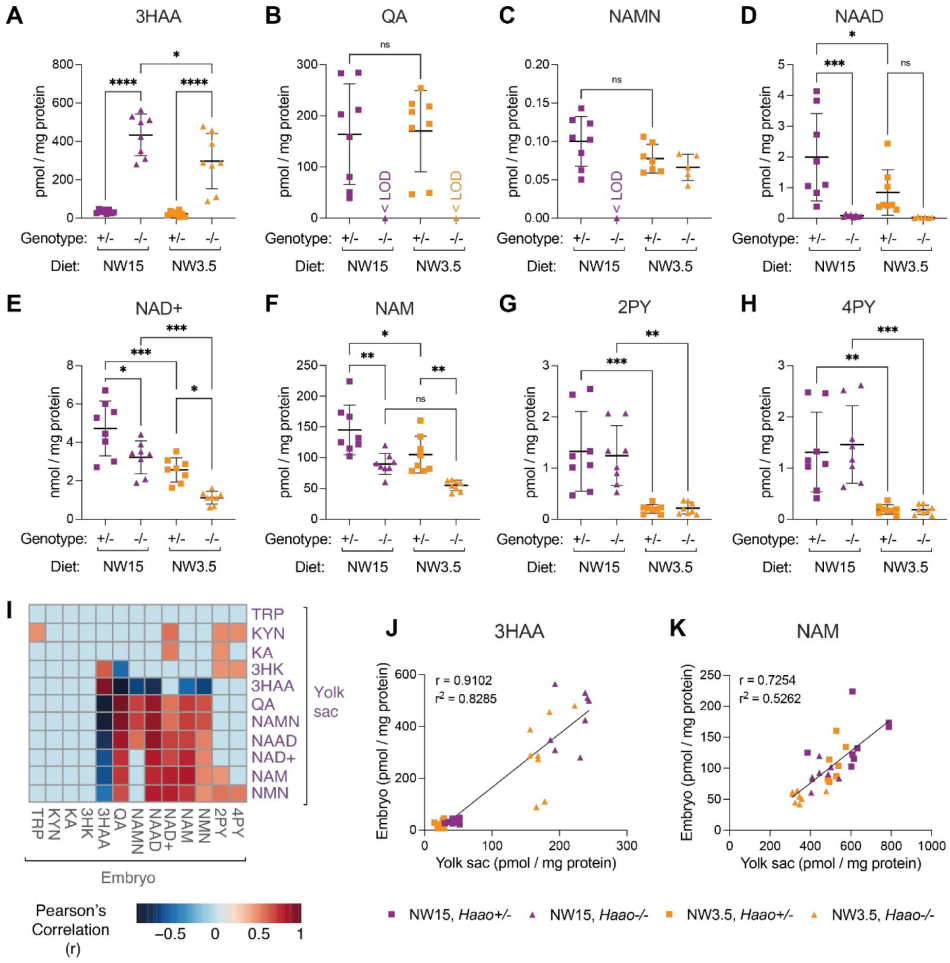


## Figure 5.

### Perturbation of yolk sac NAD metabolome at E10.5 correlates with metabolic alterations in the embryo.

(A-H) Concentration of NAD-related metabolites in E10.5 embryos normalised to total protein content. (A) 3-hydroxyanthranilic acid (3HAA), (B) quinolinic acid (QA), (C) nicotinic acid mononucleotide (NAMN), (D) nicotinic acid adenine dinucleotide (NAAD), (E) NAD+, (F) nicotinamide (NAM), (G) N-methyl-4-pyridone-5-carboxamide (4PY), (H) N-methyl-2-pyridone-5-carboxamide (2PY). Bars indicate the mean ± standard deviation. Statistical significance in (A-H) was calculated by one-way ANOVA with Tukey's multiple comparisons test with ns = not significant, * $p$<0.05, ** $p$<0.01, *** $p$<0.001, and **** $p$<0.0001. <LOD = below the limit of detection. For numerical values, see **Table S6**. (I) Heatmap showing significant Pearson's correlation ($p$ < 0.01; -0.45 < r > 0.45) between normalised metabolite levels in E10.5 yolk sacs and embryos. Correlations that did not reach significance are denoted as light blue coloured squares. (J, K) Correlation of 3HAA (J) and NAM (K) concentration in corresponding E10.5 yolk sac and embryo samples. The Pearson correlation coefficient (r) and coefficient of determination ($r^2$) are indicated in each graph. Each datapoint represents an E10.5 embryo and corresponding pooled yolk sac sample.

*Haao* genotype (3HAA, NAMN, QA and NAAD) were significantly positively correlated between the embryo and yolk sac (**Figure 5I-J**). Overall, this suggests extensive metabolite exchange between conceptus tissues occurred.

Levels of NAD Salvage Pathway metabolites NAD+, NAM and NMN were also significantly positively correlated both within and between the yolk sac and embryo tissues (**Figure 5I,K**). NAM is the main NAD precursor exported into circulation after NAD *de novo* synthesis for use in other tissues (Liu et al., 2018). Given the limited availability of other usable alternative NAD precursors in mouse circulation (Cuny et al., 2021; Liu et al., 2018), NAD levels of *Haao*$^{-/-}$ conceptuses likely depend on maternal plasma NAM (Cuny et al., 2023). Though their overall concentration markedly differed (**Table S5-6**), embryo and yolk sac NAM correlated strongly, irrespective of *Haao* genotype (**Table S5**, **Figure 5K**). Therefore, embryonic NAD status depends on NAD precursor availability in the yolk sac, which is itself determined by both maternal provision and NAD *de novo* synthesis activity.

## The yolk sac endoderm expresses requisite NAD *de novo* synthesis pathway genes at the onset of organogenesis

Having established the yolk sac as the primary site of NAD *de novo* synthesis during organogenesis and its importance in maintaining embryonic NAD levels, we next determined which cell populations are responsible for its activity by re-analysing published scRNA-seq data generated from pooled E9.5 and E10.5 yolk sacs (**Figure 6A**) (Zhao & Choi, 2019).

The yolk sac is derived from two extraembryonic lineages, the endoderm and mesoderm, which subsequently differentiate into various specialised cell types including yolk sac endoderm, vascular endothelial cells, smooth muscle cells, erythroid progenitors/cells, myeloid progenitors/cells, and macrophages (Zhao & Choi, 2019). *Tdo2* was only expressed in vascular smooth muscle cells, whereas all other NAD *de novo* Synthesis Pathway genes (*Afmid*, *Kmo*, *Kynu*, *Haao*, *Qprt* and *Nadsyn1*) were exclusively expressed in the yolk sac endoderm (**Figure 6B**). Of the *Nmnat1-3* genes, essential for all NAD biosynthesis pathways, only *Nmnat1* was expressed in the endoderm.

To establish when gene expression commenced in the endodermal lineage, we used the "extraembryonic (ExE) endoderm" population from the mouse gastrulation atlas (Pijuan-Sala et al., 2019). The tryptophan-catabolising genes *Tdo2*, *Ido1*, *Ido2* were not expressed in this population at any stage. Expression of all subsequent requisite NAD *de novo* Synthesis Pathway genes was identifiable in a subset of cells by E8 and increased thereafter (**Figure 6C**). While histological methods such as *in situ* hybridisation would be required to confirm the exact cell types expressing these genes, the available expression data indicates that the genes encoding those enzymes required to convert L-kynurenine to NAD (kynurenine pathway) are exclusively expressed in the yolk sac endoderm lineage from the onset of organogenesis (E8.0-8.5). Given the lack of *Tdo2* and *Ido2* expression across all timepoints assessed (**Figure 6B,C**), it appears the conversion of tryptophan to kynurenine is either occurring in the yolk sac vascular smooth muscle, or in the placenta which is well known to perform this function in mouse (Spinelli et al., 2018) and humans (Broekhuizen et al., 2021; Sedlmayr et al., 2014).

## NAD *de novo* synthesis pathway gene expression dynamics in humans parallel those in mice

Despite the structural differences between the mouse yolk sac and its human equivalent, the definitive secondary yolk sac (Ross & Boroviak, 2020), there is increasing evidence that many metabolic pathways are conserved in the endodermal cell population (Cindrova-Davies et al., 2017; Goh et al., 2023). Despite very different timescales of embryogenesis between the two species, the human yolk sac is present throughout organogenesis, the period when embryos are

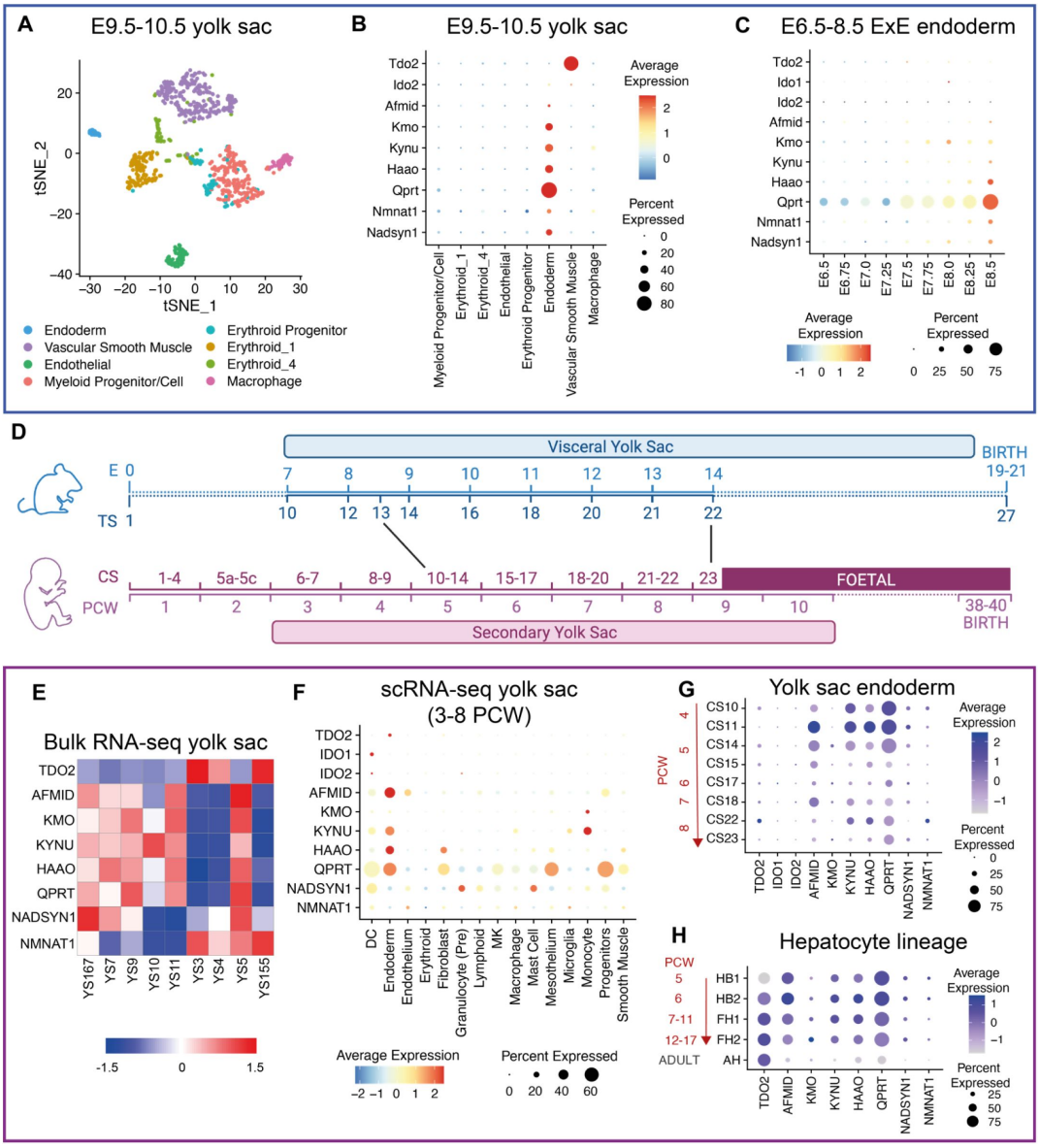


## Figure 6

**The extraembryonic endoderm and subsequent yolk sac endoderm express NAD *de novo* Synthesis Pathway genes before expression commences in the embryonic liver, in both mouse and human.**

(A) t-SNE projection of re-analysed single-cell RNA-seq data from pooled E9.5 and E10.5 visceral yolk sacs previously generated by Zhao and Choi (Zhao & Choi, 2019). (B) DotPlot showing average expression (heatmap colour) and proportion of cells (circle size) of essential NAD *de novo* Synthesis Pathway genes in E9.5/E10.5 yolk sac populations. (C) DotPlot for essential NAD *de novo* Synthesis Pathway genes in the extraembryonic endoderm (ExE) population of the mouse gastrulation atlas (Pijuan-Sala et al., 2019) from E6.5 to E8.5. (D) Schematic timeline comparing organogenesis length and yolk sac duration during mouse and human development. Stages and equivalences are approximations based on figures from *https://hdbratlas.org/comparison-HvM.html* and published staging criteria (Kaufman, 1992; O'Rahilly & Müller, 2010) (E) Heatmap showing z-normalised expression of NAD *de novo* Synthesis Pathway genes in re-analysed bulk RNA-seq samples for individual human yolk sacs, published in Cindrova-Davies et al. (Cindrova-Davies et al., 2017). (F) DotPlot for requisite NAD *de novo* Synthesis Pathway gene expression in human yolk sac populations between 3-8 post-conceptional weeks (PCW). scRNA-seq data acquired from Goh et al. (Goh et al., 2023) and re-analysed. (G) DotPlot of pathway gene expression in human yolk sac endoderm population between 3-8 PCW. (H) DotPlot of human hepatocyte lineage previously published in Wesley et al. (Wesley et al., 2022). ExE endoderm = extraembryonic endoderm, CS = Carnegie Stage, HB = hepatoblast, FH = foetal hepatocytes, AH = adult hepatocytes.

most susceptible to malformation (Alwan & Chambers, 2015), after which it degenerates and is lost (**Figure 6D**). Therefore, we investigated whether NAD *de novo* synthesis is among the conserved metabolic pathways between the two species. We examined expression of the pathway requisite genes by re-analysing bulk and scRNA-seq for the human yolk sac (Cindrova-Davies et al., 2017; Goh et al., 2023) and hepatocyte lineage (Wesley et al., 2022).

All NAD *de novo* Synthesis Pathway genes were expressed within at least one human yolk sac bulk RNA-seq sample (Cindrova-Davies et al., 2017) (**Figure 6E**), but there were significant differences in transcript levels between them. High *TDO2* expressing yolk sacs concurrently expressed *NMNAT1*, and to a lesser extent *NADSYN1* (3/9), but showed limited expression of the other requisite genes. Conversely, low *TDO2* expression yolk sacs more robustly expressed *AFMID*, *KMO*, *KYNU*, *HAAO*, *QPRT*, and *NADSYN1* (**Figure 6E**).

Re-analysis of published human scRNA-seq yolk sac data generated across organogenesis (Goh et al., 2023) showed that unlike in mice, requisite genes were expressed in multiple populations (**Figure 6F**). *KMO* expression was limited in the endoderm, with more robust expression observed in monocytes. Similarly, *NADSYN1* transcripts were more abundant in various immune cell populations. Yet, expression of *TDO2*, *AFMID*, *KYNU*, *HAAO* and *QPRT* was highest in the endodermal population (**Figure 6F**). As in mice, the proportion of endoderm cells and overall expression of *AFMID*, *KYNU*, *HAAO* and *QPRT* declined during organogenesis, with expression highest at Carnegie Stage (CS) 11 (4 post-conceptional weeks (PCW)) (**Figure 6G**). *TDO2* expression, not observed in the mouse yolk sac endoderm, increased as organogenesis progressed.

By contrast, in the hepatocyte lineage (Wesley et al., 2022), every NAD *de novo* synthesis pathway gene was expressed by 5 PCW (hepatoblast (HB) stages 1 and 2) (**Figure 6H**) and remained constant throughout foetal hepatocyte stages (FH) 1 (7-11 PCW) and 2 (12-17 PCW). Indeed, expression during embryonic stages was higher than in adult hepatocytes.

Therefore, requisite NAD *de novo* synthesis gene expression dynamics in humans largely recapitulate findings in mice with the pathway primarily active in the yolk sac endodermal cells during early organogenesis. As expression declines in this population, it increases in the hepatocyte lineage. The only major difference between the species is whether NAD *de novo* Synthesis Pathway activity in the embryonic liver is established during or after organogenesis, respectively.

## Discussion

NAD deficiency during human and mouse development causes CNDD characterised by multiple congenital malformations and foetal loss (Cuny et al., 2023; Cuny et al., 2020; Dunwoodie et al., 2023; Mark & Dunwoodie, 2023; Shi et al., 2017; Szot et al., 2020; Szot et al., 2024; Szot et al., 2021). Human CNDD cases are characterised by biallelic pathogenic variants in either *KYNU*, *HAAO* or *NADSYN1*, all genes of the NAD *de novo* Synthesis Pathway. Mouse models of CNDD demonstrate that NAD *de novo* synthesis occurs in the conceptus and that this activity is required for normal embryonic development unless the mother provides sufficient vitamin B3 which bypasses NAD *de novo* synthesis (Shi et al., 2017). Here we report that NAD *de novo* synthesis occurs at two sites in the conceptus; first in the transient extra-embryonic yolk sac during organogenesis, and later in the embryonic liver once formed. It is noteworthy that the placenta lacks this activity. We present evidence in human gene expression data that the NAD *de novo* Synthesis Pathway also occurs initially in the secondary yolk sac and later in the embryonic liver. Until now, the site of NAD *de novo* synthesis in the mammalian conceptus was unknown. The necessity of this metabolic activity in the yolk sac highlights the importance of this transient tissue in mammalian embryogenesis.

## The murine yolk sac is capable of synthesising NAD de novo

The yolk sac has various important functions during embryogenesis, including the uptake and processing of macro-and micronutrients before and after the formation of a functional chorioallanotic placenta. It also facilitates the transport of maternal lipids, cholesterol and other metabolites to the embryo until the embryonic liver can take over this function, and it is involved in haematopoiesis and gene regulation (Cindrova-Davies et al., 2017). Furthermore, the yolk sac metabolises teratogenic substances (Terlouw & Bechter, 1992). Disruption of yolk sac function causes embryonic malformation phenotypes that overlap with CNDD (Brent & Fawcett, 1998; Brent et al., 1971; Ornoy & Miller, 2023; Perez-Garcia et al., 2018), underscoring the yolk sac's crucial role for normal embryo development.

Our finding of NAD *de novo* synthesis activity as another metabolic process of the yolk sac is notable because it represents a multi-step pathway involving several sequential enzyme-catalysed processes. Our RNA-seq data analysis confirms that all requisite genes required for NAD *de novo* synthesis from kynurenine are expressed in mouse yolk sac endoderm cells. *Tdo2*, required for the conversion of tryptophan to kynurenine, is expressed in the adjacent vascular smooth muscle cells. Our HAAO enzymatic assays and metabolic analyses confirm the pathway is indeed functional. Therefore, this is the first demonstration of NAD *de novo* synthesis occurring in a tissue outside of the liver and kidney.

## NAD deficiency in early organogenesis is sufficient to cause CNDD

We developed a refined CNDD model by which we modulated the maternal dietary NAD precursor supply during a 3-day window between E7.5 to E10.5 to be either low (NW3.5) or sufficient (NW15). Combined with maternal *Haao*$^{-/-}$and paternal *Haao*$^{+/-}$ genotype, the NW3.5 diet reproducibly generated *Haao*$^{-/-}$ embryos with malformations and unaffected *Haao*$^{+/-}$ littermates. The *Haao*$^{-/-}$ embryos exhibited a spectrum of CNDD defects but no cleft palate seen in our previous study with a precursor restriction for five days between E7.5 and E12.5 (Shi et al., 2017). The absence of palate defects is possibly because our current 3-day dietary precursor-restriction is too short to perturb the later occurring developmental processes of palate formation. This observation supports our hypothesis that the timing of NAD deficiency during organogenesis determines which organs/tissues are affected (Cuny et al., 2023), but more research is needed to fully characterise the onset and duration of embryonic NAD deficiency in dietary NAD precursor restriction mouse models.

Furthermore, diminished NAD *de novo* synthesis in the yolk sac is responsible for the defects caused by our 3-day precursor restriction, because the embryonic liver has not yet formed. These data indicate that the timing of NAD deficiency determines whether tissues known to be susceptible to CNDD are affected or not, explaining why phenotypes are highly variable within the CNDD spectrum. But it is currently unknown whether a common underlying molecular mechanism exists that unifies these tissues with respect to their disrupted development in CNDD and whether organs/tissues that are seemingly unaffected by NAD deficiency are resistant to this mechanism. Further research into the molecular and cellular effects of altered NAD availability during organogenesis is required to better understand CNDD causation.

## Maternal vitamin B3 early in pregnancy can overcome a genetic disruption of yolk sac NAD de novo synthesis

The most abundant NAD precursors in circulation are L-tryptophan, L-kynurenine, and NAM (Cuny et al., 2020; Liu et al., 2018). Flux experiments in mice confirmed that the liver converts L-tryptophan into NAM and excretes it into circulation to maintain NAD levels using the NAD Salvage Pathway (Liu et al., 2018). The CNDD models employed here use *Haao*$^{-/-}$ mothers, who along with their *Haao*$^{-/-}$ embryos, cannot use the L-tryptophan provided. These *Haao*$^{-/-}$ mothers

and embryos are instead dependent on the vitamin B3 provided in the diet to synthesise NAD. The amount provided in the NW15 diet is sufficient to maintain conceptal NAD levels and normal embryonic development. By contrast, on the more vitamin B3 restricted NW3.5 diet, the ability to perform NAD *de novo* synthesis using the L-tryptophan is ultimately what distinguishes the unaffected *Haao*$^{+/-}$ embryos from their affected *Haao*$^{-/-}$ littermates.

Indeed, *Haao*$^{-/-}$ yolk sacs had lowered NAD levels under both diets, but the lowest NAD levels were found in NW3.5 *Haao*$^{-/-}$ yolk sacs with the combination of genetic block of NAD *de novo* synthesis and dietary NAD precursor restriction. Similarly, embryonic NAD levels significantly declined under genetic block (*Haao*$^{-/-}$, NW15) or vitamin B3 restriction (*Haao*$^{+/-}$, NW3.5) alone relative to *Haao*$^{+/-}$on the NW15 diet but these were still sufficient to maintain normal development. By contrast, those embryos that would go on to develop defects, *Haao*$^{-/-}$embryos on NW3.5, had the lowest NAD levels at E10.5, as observed previously (Cuny et al., 2020; Shi et al., 2017). This underscores that NAD deficiency in the embryo is linked to the inability of the yolk sac to perform NAD *de novo* synthesis from maternally provided precursors.

Though unaffected by the *Haao* genetic block, the Preiss-Handler Pathway (**Figure 1A**) does not appear to play a role in yolk sac NAD synthesis given that the relevant metabolites NAMN and NAAD were undetectable or negligible in *Haao*$^{-/-}$ yolk sacs regardless of diet. This leaves the NAD Salvage Pathway, and its circulatory precursor NAM, as the main source of NAD in *Haao*$^{-/-}$ yolk sacs, as well as their corresponding embryos, as suggested previously (Cuny et al., 2023; Szot et al., 2024). Indeed, NAM levels were lower in *Haao*$^{-/-}$ yolk sacs compared to *Haao*$^{+/-}$ under the equivalent diet, and yolk sac NAM levels strongly correlated with embryonic NAM in corresponding embryos irrespective of condition. Though not significantly different, the increase in NAM levels in both *Haao*$^{-/-}$ tissues on the NW15 diet over the NW3.5 diet, and the corresponding significant increase in NAD levels themselves, likely originates from the additional provision of NAM from the mother under this diet. Correspondingly, levels of excretion products 2PY and 4PY, which are generated from NAM (**Figure 1A**) when its levels are in excess, were significantly lowered and close to zero in E10.5 *Haao*$^{-/-}$ embryos on NW3.5 relative to NW15 embryos, indicating a low to insufficient NAD status.

Besides the direct effect of embryonic NAD deficiency as the cause of CNDD, it is possible that the low NAD levels observed in the yolk sac under NW3.5 diet also interfere with other crucial yolk sac functions that are linked to NAD, such as ATP-dependent active transport of essential nutrients (Chang, 2010; Cindrova-Davies et al., 2017; Dutta & Sinha, 2017) or NADP-dependent enzymes (Di Pietro et al., 2002; Xiao et al., 2018), thereby further impacting normal embryonic development. Likely, it is a combination of both. Determining the specific mechanisms of CNDD causation requires further studies.

Together, our NAD metabolome findings confirm that if vitamin B3 supply is limited, yolk sac NAD *de novo* synthesis becomes essential for maintaining NAD and normal embryo development. Further work with more refined analytical approaches, such as molecular flux analysis, could determine to which extent specific metabolites are exchanged between maternal circulation, the yolk sac, and the embryo.

## Yolk sac functions, very likely including NAD de novo synthesis, are conserved in human

Human embryogenesis requires a transient primary (day 7 to day 12) and secondary yolk sac (day 13 to day 49), while the mouse has a single yolk sac (E7.5 to birth). While human yolk sac anatomy and the timing of its presence differs to mouse, many functions are conserved between the species. These functions include serum protein synthesis, micro- and macronutrient transportation, and certain metabolic pathways, and it is also the site of primary haematopoiesis (Cindrova-Davies et al., 2017). Using published datasets, we showed that the human yolk sac

expresses all genes required for NAD *de novo* synthesis during comparable embryonic stages as seen in the mouse. Therefore, it is plausible that yolk sac NAD *de novo* synthesis activity in early pregnancy is of similar importance to maintain NAD status and allow normal embryonic development in humans.

Recent studies have established a link between human yolk sac disruption and adverse pregnancy outcomes. Specifically, a disruption of yolk sac size and shape in the first trimester was a predictor of foetal anomalies and pregnancy loss (Cho et al., 2006; Detti et al., 2021; Marin et al., 2021; Suguna & Sukanya, 2019). Maternal diabetes during pregnancy is also a known risk factor for congenital anomalies (Gabbay-Benziv et al., 2015). Recent studies suggest that maternal diabetes not only affects the embryo but also the yolk sac due to hyperglycaemia, impairing nutrient transportation that drives embryopathy (Dong et al., 2016; Reece et al., 1994). Furthermore, diabetes has been implicated in perturbations of the NAD *de novo* Synthesis Pathway (Allegri et al., 2003; Liu et al., 2019; Oxenkrug, 2015). Therefore, it is possible that disruption of NAD *de novo* synthesis, either maternally or in the yolk sac itself, may contribute to the formation of congenital malformations under diabetic conditions.

Furthermore, it is possible that the yolk sac NAD *de novo* synthesis capability is also conserved in non-mammalian vertebrates. At least one step of the pathway, catalysed by AFMID (**Figure 1A**), was found to be active in chicken egg yolk sac membranes (Seifert, 2017). Inhibition of this enzyme in the yolk sac resulted in lowered embryo NAD levels and some evidence of disrupted embryogenesis (Seifert & Casida, 1978; Seifert & Casida, 1979). Whether the entire NAD *de novo* Synthesis Pathway is active in the avian yolk sac, or whether downstream enzymatic synthesis steps are performed elsewhere, is unclear and requires further research.

### Outlook

We have shown in mice that NAD deficiency due to an impaired NAD *de novo* Synthesis Pathway can be prevented by supplementing pregnant mice with the NAD precursor vitamin B3 (Cuny et al., 2020; Shi et al., 2017; Szot et al., 2024). NAD deficiency between E7.5 and 10.5 recapitulates the majority of CNDD malformations, and under more severe conditions from E0.5 to 3.5 all embryos die (Shi et al., 2017). These mouse stages span approximately days 1 to 17 of human development (**Figure 6D**). Therefore, in women at risk of becoming NAD deficient, it would be necessary to enter pregnancy with sufficient NAD by taking vitamin B3 prior to pregnancy. Further research on the molecular intricacies of CNDD causation, the timing, and the tissues and cells involved will aid understanding of the causes of birth defects and miscarriages more generally.

Here, we highlight the importance of the yolk sac in embryogenesis. Given the link between yolk sac changes and miscarriage are established, other environmental and/or genetic factors may perturb yolk sac function and drive congenital malformation and embryo loss. Whilst CNDD should be preventable through supplementation, other causes may not be and instead require other approaches. Further research is required to better understand the mechanisms of CNDD causation and of other causes of adverse pregnancy outcomes involving the yolk sac.

## Materials and methods

### Animal experiments

All animal experiments were performed in accordance with protocols approved by the Garvan Institute of Medical Research/St. Vincent's Animal Experimentation Ethics Committee, Sydney, Australia (approvals 18/27 and 21/18). The *Haao* loss-of-function mouse line (allele $Haao^{em1Dunw}$) has been described previously (Shi et al., 2017).

Mice were maintained on Breeder diet (Rat and Mouse Premium Breeder Diet, Gordons Specialty Feeds, Bargo, Australia) containing 90 mg/kg niacin and 3.7 g/kg L-tryptophan. Mice were set up for timed matings and pregnancy was confirmed by the presence of a vaginal copulation plug in the morning (defined as timepoint E0.5). Pregnant females were culled between E10.5 and E18.5 by cervical dislocation and embryos dissected. From each embryo, the following tissues were collected: whole visceral yolk sac, placenta (whole placenta at E10.5-11.5, ½ placenta at E12.5-13.5, ¼ placenta at E14.5-18.5), and whole embryonic liver. All embryonic tissues were weighed prior to being snap frozen in liquid nitrogen. Tissues were genotyped for the *Haao* loss-of-functional allele as described previously (Cuny et al., 2020; Shi et al., 2017).

For experiments requiring limitation of the maternal dietary vitamin B3 supply during critical organogenesis stages, pregnant females were maintained on Breeder diet until E7.5. Between E7.5 and E10.5, the females were temporarily housed in a new cage and provided a diet lacking any NAD precursors (SF21-083, Specialty feeds) and drinking water containing 1 g/L L-tryptophan and 3.5 mg/L nicotinic acid (NW3.5) or 15 mg/L (NW15). At E10.5, females were re-placed on Breeder diet until embryo dissection.

E18.5 embryos were phenotyped as described previously (Cuny et al., 2020) except for the identification of heart defects, for which micro-CT was used. Briefly, hearts were dissected from fixed (4% paraformaldehyde with 1% glutaraldehyde) E18.5 embryos and stained in 0.7% phosphotungstic acid + 30% ethanol in phosphate-buffered saline (PBS) for a minimum of 7 days or until stained completely. Stained hearts were scanned using a Skyscan 1272 scanner (Bruker Corporation, Billerica, USA) at a resolution of 1092×1632 with a voltage of 80 kV and a 125 µA current. The filter was set to Al 1 mm with a pixel size of 4.95 µm. Projection images were recorded with 2300 ms exposure time per projection with a rotation step of 0.4° between projections. The hearts were scanned at a total of 360° rotation. Acquired projections were reconstructed using Nrecon software (Bruker) with smoothing set to 3, ring artefact reduction to 19, and beam hardening to 10%. Reconstructed volumes were exported in .TIFF format and visually inspected for structural heart defects.

## HAAO enzyme assays

HAAO enzyme assays were performed as previously described, with some minor modifications (Shi et al., 2017; Walsh et al., 1991). Briefly, volume of tissue lysis buffer (10 mM protease inhibitor in PBS) was adjusted by stage and tissue type to standardise total protein levels per assay (see Supplementary Table 1). Due to the small tissue size, yolk sacs and embryonic livers were pooled at early gestational stages to obtain sufficient material per biological replicate. Regardless of tissue type, 15 µL of tissue lysate was used per reaction and normalised by total protein per reaction. Protein concentration was determined by Pierce BCA Protein Assay Kit (Thermo Scientific, Rockford, USA), performed according to the manufacturer's protocol.

## Quantitative Real Time PCR (qRT-PCR)

RNA was extracted from snap frozen *Haao*$^{+/-}$ yolk sacs using PureLink$^{TM}$ RNA Mini kit (Thermo Scientific, Rockford, USA), as per the manufacturer's instructions. Tissue homogenization was performed in 650 µL lysis buffer using a Bio-Gen Pro 200 homogenizer (PRO Scientific Inc., Oxford, Connecticut, USA). cDNA was synthesised from 1 µg RNA using Maxima First Strand cDNA Synthesis Kit (K1672, Thermo Scientific) according to the manufacturer's protocol, with the addition of a dilution step to 1.6 ng/µL in water. qPCR was performed on CFX384 Touch Real-Time PCR Detection System (Bio-Rad, USA) using the primers detailed in **Table S7** and LightCycler 480 SYBR Green I Master mix (04887352001; Roche Holding AG). Relative expression was calculated using the ΔCt method, normalizing each gene to both *Ubc* and *Ywhaz* levels.

## Metabolite quantification by UHPLC-MS/MS

NAD+ and related metabolites were quantified in yolk sacs and placentas collected at E10.5, E12.5 and E14.5, in embryos collected at E10.5, and in embryonic livers collected at E14.5 using UHPLC-MS/MS as described for mouse liver tissue (Cuny et al., 2021), with a minor adjustment to improve quantification of high concentration metabolites. From the last supernatant after addition of chloroform and centrifugation, 30 µL were taken, diluted with 70 µL of 100 mM ammonium acetate in water (=sample for abundant metabolite quantification), and measured. The remainder of supernatant was dried in a vacuum centrifuge at room temperature, metabolites reconstituted in 60 µL of 100 mM ammonium acetate, centrifuged for 2 min at 15,000 g and 4°C, and 50 µL of the supernatant taken and measured by UHPLC-MS/MS as described (=sample for low concentration metabolite quantification). Metabolite concentration values were normalised by the tissue sample wet weight at dissection. Metabolite concentrations in NW3.5 and NW15 embryos and yolk sacs were additionally normalised by protein concentration in the solid fraction (pellet) remaining after the first centrifugation step of the metabolite extraction procedure. To determine total protein concentration in the pellets, they were washed in methanol, air dried using a vacuum centrifuge, resuspended in 0.2 M sodium hydroxide, and incubated at 95°C for 20 minutes. Insoluble proteins and other debris were removed by centrifugation at 12000 rpm for 7 minutes in a microcentrifuge and protein concentration was determined using the Pierce BCA Protein Assay Kit (Thermo Scientific, Rockford, USA) according to the manufacturer's protocol.

## Analysis of published RNA-seq datasets

RNA-Seq datasets (matrix tables for single cell and fastq for bulk RNA-Seq) were downloaded from public repositories (**Table S8**). For the re-analysis of bulk RNA sequencing fastq files were trimmed of low quality sequence and adaptor using Trimmomatic (v0.35) (Bolger et al., 2014) before being aligned to hg38 genome using the STAR aligner (two pass method) (Dobin et al., 2013). Gene counts were generated from the STAR aligner using gencode vM10 as the reference gene model. Gene count matrixes were assembled genes expressed at 1 count per million (CPM) in at least 3 samples and were normalised by Trimmed Mean of M-values (TMM) and log2 transformed.

For the re-analysis of single cell datasets, single cell count matrixes were downloaded and assembled into Seurat objects using the Seurat R package (Butler et al., 2018). Cells were filtered for percent of mitochondrial content, and clustering included detection of top variable genes, scaling, dimensionality reduction with PCA and construction of nearest neighbour graphs. Cell cluster identification was established from markers described in linked manuscript (**Table S8**). For the gastrulation atlas – single cell count objects were downloaded from the Bioconductor "MouseGastrulationData" resource (Griffiths & Lun, 2023).

## Statistical Analysis

One-way ANOVA was used to determine statistical significance of tissue sample gene expression levels at different developmental stages, of HAAO activity in tissues of different *Haao* genotypes, and of metabolite concentrations under different *Haao* genotypes and maternal diets. Significance of metabolite level differences was additionally analysed by one-way ANOVA with Tukey's multiple comparisons test. Student's t-test was used to determine statistical difference of $Haao^{+/-}$ and $Haao^{-/-}$ embryo weights with the NW3.5 diet. Values are displayed as mean ± standard deviation. All statistical analyses were performed with Prism (version 10; GraphPad Software). Metaboanalyst 5.0 (Pang et al., 2022) was used to generate PCA plots and heatmaps of the NAD metabolome data. Custom R scripts were used to generate heatmaps of gene expression data.

# Supplementary figures and tables

## Figure S1.

**RidgePlots show that the time of onset, expression level, and proportion of hepatocyte-lineage cells expressing NAD *de novo* synthesis genes varies, including for *Kmo* (A), *Kynu* (B), *Haao* (C) and *Qprt* (D) from E9.5 to E15.5.**

Data previously generated in Mu et al. (Mu et al., 2020).

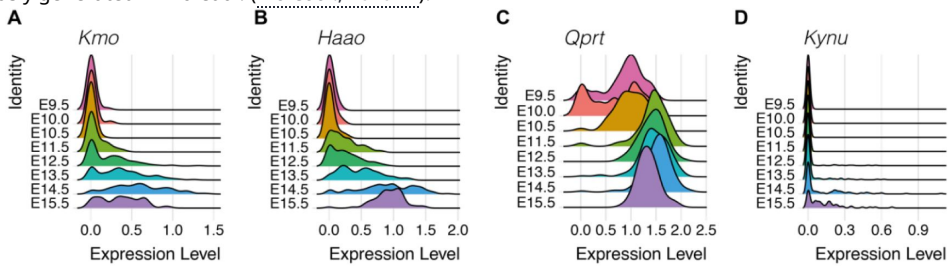


## Figure S2.

**The mouse embryo has negligible HAAO enzyme activity and thus lacks NAD *de novo* synthesis capability until it has developed a liver.**

(A) HAAO enzyme activity in whole embryo, placenta, and yolk sac at E11.5. (B) HAAO enzyme activity in embryo with its liver removed, isolated embryonic liver, placenta, and yolk sac at E14.5. The mice to generate dataset (B) were maintained on AIN93G diet (Specialty Feeds, Glen Forrest, Australia) which, while different to the Breeder diet used in the other experiments, provides sufficient NAD precursors for normal development (Cuny et al., 2023). Statistical significance was determined by one-way ANOVA with Tukey's multiple comparisons test with * $p<0.05$; ** $p<0.01$; *** $p<0.001$; **** $p<0.0001$. Bars indicate the mean ± standard deviation.

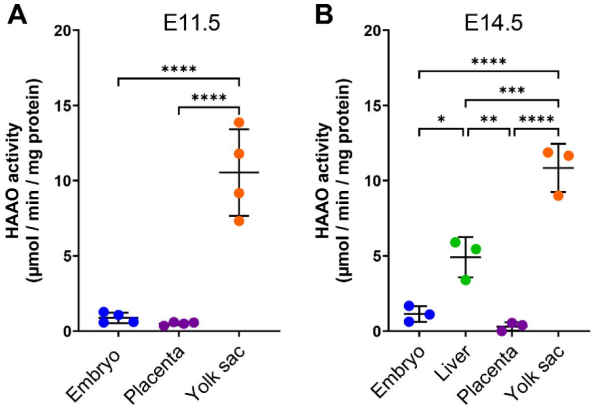

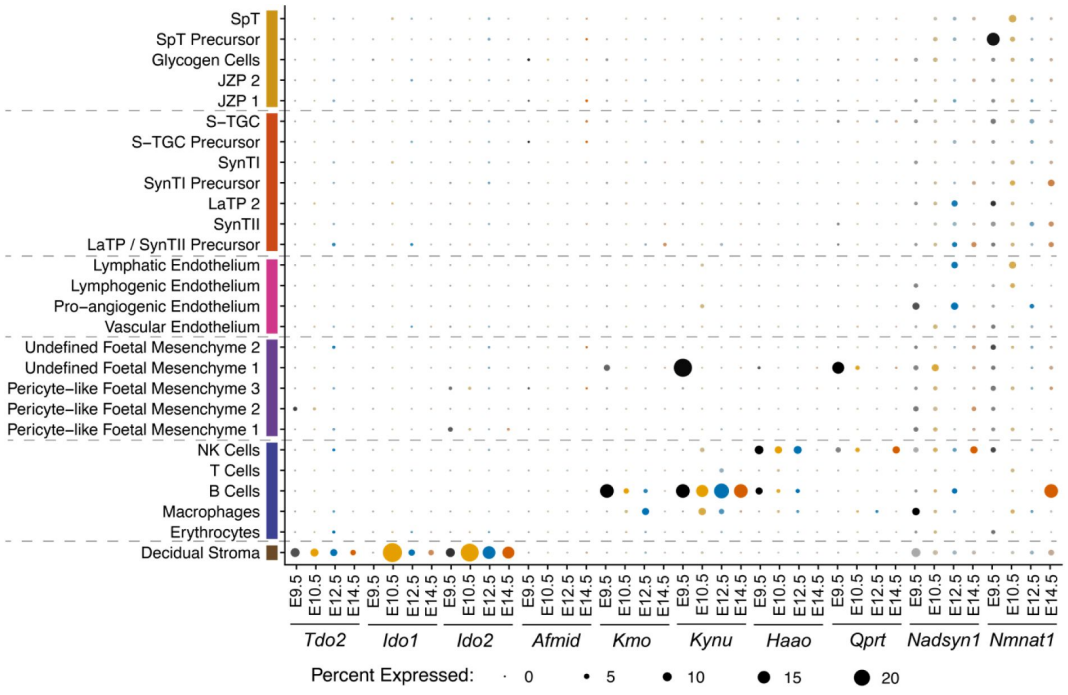


## Figure S3.

### NAD *de novo* Synthesis Pathway activity is absent from the mouse placenta.

DotPlot showing proportion of cells (circle size) expressing requisite pathway genes in different placental cell populations at E9.5 (black), E10.5 (yellow), E12.5 (blue) and E14.5 (orange) using scRNA-seq generated by Marsh and Blelloch (Marsh & Blelloch, 2020). Placental populations were clustered by lineage: junctional zone trophoblast (yellow), labyrinth layer trophoblast (orange), endothelium (pink), mesenchyme (purple), immune/blood cells (indigo), and maternal decidual stroma (brown).

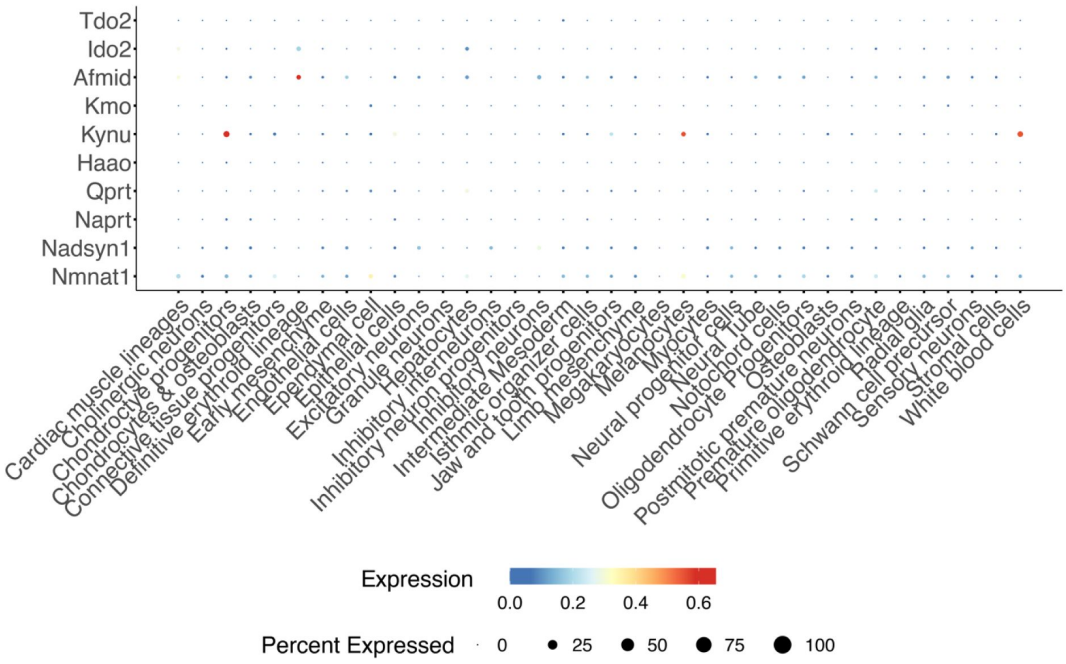


**Figure S4.**

**NAD *de novo* Synthesis Pathway gene expression is negligible in the E10.5 embryo.**

DotPlot shows the proportion of cells (circle size) expressing requisite pathway genes in E10.5 embryo cell populations. scRNA-seq generated as part of the 'mouse organogenesis cell atlas' (MOCA) by Cao et al. (Cao et al., 2019) and analysed using ShinyCell (Ouyang et al., 2021). Gene expression data is not scaled.

## Table S1.

**HAAO enzyme activity in embryonic liver, yolk sac, placenta, and embryo at different stages in gestation.**

| Tissue | Stage | # | Vol. buffer / mg weight | HAAO activity (μmol min$^{-1}$ mg protein$^{-1}$) *Haao+/+* | n | *Haao+/-* | n | *Haao-/-* | n | One-way ANOVA *p* |
|---|---|---|---|---|---|---|---|---|---|---|
| Embryonic liver | E12.5 | 4-7 | 3 μL | 0.76 ± 0.04 | 4 | 0.62 ± 0.19 | 4 | 0.46 ± 0.07 | 3 | 0.0383 |
| | E13.5 | 2-3 | 3 μL | 1.70 ± 0.54 | 4 | 1.49 ± 0.42 | 4 | 0.45 ± 0.08 | 4 | 0.0034 |
| | E14.5 | 1 | 4 μL | 3.30 ± 0.17 | 4 | 2.15 ± 0.17 | 4 | 0.69 ± 0.25 | 4 | <0.0001 |
| | E15.5 | 1 | 4 μL | 4.77 ± 0.68 | 4 | 2.99 ± 0.87 | 5 | 0.29 ± 0.13 | 4 | <0.0001 |
| | E16.5 | 1 | 4 μL | 8.82 ± 2.03 | 4 | 4.66 ± 1.55 | 4 | 0.44 ± 0.04 | 4 | <0.0001 |
| | E17.5 | 1 | 5 μL | 15.64 ± 4.21 | 4 | 8.45 ± 3.65 | 4 | 0.47 ± 0.06 | 4 | <0.0001 |
| Yolk sac | E11.5 | 2-3 | 3 μL | 10.73 ± 3.89 | 4 | 5.75 ± 1.39 | 4 | 0.12 ± 0.83 | 4 | 0.0006 |
| | E12.5 | 1-2 | 3 μL | 10.68 ± 3.38 | 4 | 5.76 ± 2.20 | 4 | 0.35 ± 0.35 | 4 | 0.0005 |
| | E13.5 | 1 | 3.5 μL | 11.35 ±2.89 | 4 | 5.95 ± 1.45 | 5 | 0.48 ± 0.14 | 4 | <0.0001 |
| | E14.5 | 1 | 4 μL | 8.87 ± 2.49 | 4 | 4.22 ± 0.34 | 4 | 0.50 ± 0.22 | 4 | <0.0001 |
| | E15.5 | 1 | 4 μL | 5.19 ± 0.70 | 4 | 2.91 ± 0.78 | 5 | 0.32 ± 0.19 | 4 | <0.0001 |
| | E16.5 | 1 | 4 μL | 5.54 ± 1.03 | 4 | 2.64 ± 0.30 | 4 | 0.17 ± 0.15 | 4 | <0.0001 |
| | E17.5 | 1 | 4 μL | 4.05 ± 0.46 | 4 | 2.26 ± 0.29 | 5 | 0.25 ± 0.17 | 4 | <0.0001 |
| Placenta | E11.5 | 1 | 3 μL | 0.49 ± 0.19 | 4 | 0.37 ± 0.02 | 4 | 0.49 ± 0.16 | 4 | 0.3952 |
| | E12.5 | 1 | 4.5 μL | 0.32 ± 0.09 | 4 | 0.42 ± 0.09 | 4 | 0.44 ± 0.11 | 4 | 0.2221 |
| | E13.5 | 1 | 4.5 μL | 0.43 ± 0.17 | 4 | 0.32 ± 0.12 | 4 | 0.44 ± 0.07 | 4 | 0.3593 |
| | E14.5 | 1 | 4.5 μL | 0.42 ± 0.06 | 4 | 0.55 ± 0.14 | 4 | 0.44 ± 0.18 | 4 | 0.3907 |
| | E15.5 | 1 | 5 μL | 0.40 ± 0.25 | 4 | 0.48 ± 0.23 | 4 | 0.49 ± 0.27 | 4 | 0.8401 |
| | E16.5 | 1 | 5 μL | 0.50 ± 0.26 | 4 | 0.50 ± 0.10 | 4 | 0.53 ± 0.28 | 4 | 0.9739 |
| | E17.5 | 1 | 5 μL | 0.44 ± 0.03 | 4 | 0.45 ± 0.19 | 4 | 0.53 ± 0.10 | 4 | 0.5795 |
| Embryo | E11.5 | 1 | 2.5 μL | 0.88 ± 0.34 | 4 | n.d. | | n.d. | | |

E = embryonic day; # = number of samples pooled per biological replicate; n = number of biological replicates. Data shown as mean ± standard deviation. Statistical significance was calculated by one-way ANOVA comparing the three *Haao* genotypes at each embryonic stage. n.d. = not determined.

## Table S2.

**NAD metabolite concentrations in embryonic liver at E14.5 by *Haao* genotype, as measured by UHPLC-MS/MS.**

| Metabolite | *Haao+/+* | *Haao+/−* | *Haao−/−* | *p*[b] |
|---|---|---|---|---|
| TRP (nmol/g) | 77.3 ± 4.9 | 62.4 ± 34 | 81.7 ± 18.3 | 0.4932 |
| KYN (nmol/g) | 6.35 ± 0.58 | 5.11 ± 1.79 | 6.19 ± 2.14 | 0.6494 |
| 3HK (nmol/g) | 0.67 ± 0.08 | 0.66 ± 0.17 | 0.95 ± 0.17 | **0.0447** |
| 3HAA (nmol/g) | 0.11 ± 0.03 | 0.70 ± 0.97 | 5.09 ± 2.73 | **0.0141** |
| QA (nmol/g) | 2.25 ± 0.38 | 3.15 ± 0.98 | <LOD | n.a. |
| NAMN (pmol/g) | 33.0 ± 6.36 | 39.1 ± 27.1 | 6.12 ± 1.65 | 0.0951 |
| NAD+ (nmol/g) | 96.0 ± 4.2 | 81.2 ± 9.2 | 53.0 ± 7.6 | **0.0001** |
| NAM (nmol/g) | 20.9 ± 5.5 | 19.7 ± 7.3 | 39.8 ± 12.3 | **0.0325** |
| NMN (nmol/g) | 0.35 ± 0.06 | 0.31 ± 0.15 | 0.42 ± 0.10 | 0.3660 |
| 2PY (nmol/g) | 0.34 ± 0.11 | 0.16 ± 0.23 | 0.38 ± 0.20 | 0.3020 |
| 4PY (nmol/g) | 0.43 ± 0.16 | 0.20 ± 0.31 | 0.47 ± 0.25 | 0.2257 |
| KA (pmol/g) | 93.7 ± 26.7 | 78.2 ± 35.6 | 95.3 ± 26.3 | 0.7123 |
| KYN : TRP[a] | 0.08 ± 0.02 | 0.09 ± 0.02 | 0.08 ± 0.02 | 0.6246 |

Metabolite concentrations are normalised to wet weight measured at dissection. TRP = L-tryptophan; KYN = L-kynurenine; 3HK = 3-hydroxykynurenine; 3HAA = 3-hydroxyanthranilic acid; QA = quinolinic acid; NAMN = nicotinic acid mononucleotide; NAD+ = nicotinamide adenine dinucleotide; NAM = nicotinamide; NMN = nicotinamide mononucleotide; 2PY = N-methyl-2-pyridone-5-carboxamide; 4PY = N-methyl-4-pyridone-5-carboxamide; KA = kynurenic acid. Number of biological replicates is n = 3 for *Haao*$^{+/+}$ and *Haao*$^{+/-}$, n = 5 for *Haao*$^{-/-}$. Data is shown as mean ± standard deviation. <LOD = below the detection limit (signal:noise <3). n.a. = not applicable (significance cannot be calculated).

[a]KYN:TRP ratio was calculated for individual samples, then summarised.

[b]Statistical significance was calculated by one-way ANOVA comparing the three *Haao* genotypes, with $p<0.05$ highlighted in bold.

| Metabolite | Stage | Yolk sac | | | |
|---|---|---|---|---|---|
| | | +/+ | +/− | −/− | $p^b$ |
| TRP (nmol/g) | E10.5 | 49.7 ± 9.5 | 61.7 ± 12.7 | 72.0 ± 17.8 | 0.1822 |
| | E12.5 | 150 ± 42 | 133 ± 23 | 161.8 ± 35 | 0.5446 |
| | E14.5 | 159 ± 14 | 149 ± 38 | 145 ± 33 | 0.8105 |
| KYN (nmol/g) | E10.5 | 7.3 ± 2.0 | 9.3 ± 3.7 | 11.4 ± 2.8 | 0.2160 |
| | E12.5 | 37.3 ± 6.1 | 43.4 ± 1.7 | 39.8 ± 5.8 | 0.3917 |
| | E14.5 | 49.9 ± 7.0 | 62.6 ± 21.0 | 58.7 ± 9.7 | 0.5033 |
| 3HK (nmol/g) | E10.5 | 0.26 ± 0.14 | 0.48 ± 0.27 | 0.83 ± 0.38 | 0.0839 |
| | E12.5 | 1.07 ± 0.38 | 0.82 ± 0.42 | 3.30 ± 1.05 | **0.0039** |
| | E14.5 | 0.74 ± 0.25 | 0.74 ± 0.28 | 0.84 ± 0.18 | 0.7414 |
| 3HAA (nmol/g) | E10.5 | <LOD | <LOD | 6.2 ± 1.45 | n.a. |
| | E12.5 | 0.40 ± 0.11 | 0.69 ± 0.03 | 12.5 ± 3.4 | **0.0022** |
| | E14.5 | 0.21 ± 0.07 | 0.33 ± 0.09 | 5.19 ± 0.55 | **<0.0001** |
| NAMN (nmol/g) | E10.5 | 0.20 ± 0.04 | 0.39 ± 0.22 | <LOD | n.a. |
| | E12.5 | 0.80 ± 0.44 | 1.10 ± 0.65 | <LOD | n.a. |
| | E14.5 | 0.50 ± 0.09 | 0.62 ± 0.22 | 0.04 ± 0.02 | **0.0003** |
| NAD+ (nmol/g) | E10.5 | 48.7 ± 7.8 | 55.3 ± 14.3 | 50.5 ± 3.6 | 0.6304 |
| | E12.5 | 116.6 ± 17 | 99.3 ± 17.6 | 92.1 ± 7.1 | 0.0933 |
| | E14.5 | 82.9 ± 11.2 | 87.3 ± 28.1 | 83.2 ± 16.9 | 0.9501 |
| NAM (nmol/g) | E10.5 | 15.2 ± 3.4 | 13.2 ± 5.1 | 7.8 ± 1.6 | **0.0303** |
| | E12.5 | 17.2 ± 4.4 | 29.9 ± 29.5 | 19.2 ± 8.0 | 0.5815 |
| | E14.5 | 14.0 ± 3.5 | 16.9 ± 3.1 | 15.5 ± 4.9 | 0.7124 |
| NMN (nmol/g) | E10.5 | 0.28 ± 0.11 | 0.35 ± 0.18 | 0.34 ± 0.14 | 0.8232 |
| | E12.5 | 2.65 ± 0.78 | 2.84 ± 1.73 | 2.33 ± 1.41 | 0.8728 |
| | E14.5 | 3.12 ± 0.60 | 4.04 ± 0.69 | 4.25 ± 1.65 | 0.4826 |
| 2PY (nmol/g) | E10.5 | 0.13 ± 0.03 | 0.12 ± 0.03 | 0.05 ± 0.04 | **0.0215** |
| | E12.5 | 0.28 ± 0.05 | 0.17 ± 0.04 | 0.23 ± 0.09 | 0.2284 |
| | E14.5 | 0.27 ± 0.09 | 0.22 ± 0.18 | 0.25 ± 0.13 | 0.9103 |
| 4PY (nmol/g) | E10.5 | 0.16 ± 0.02 | 0.14 ± 0.03 | 0.07 ± 0.03 | **0.0083** |
| | E12.5 | 0.48 ± 0.11 | 0.28 ± 0.08 | 0.41 ± 0.15 | 0.2062 |
| | E14.5 | 0.80 ± 0.14 | 0.76 ± 0.61 | 0.75 ± 0.42 | 0.9879 |
| KA (nmol/g) | E10.5 | 0.12 ± 0.18 | 0.11 ± 0.16 | 0.14 ± 0.38 | 0.4329 |
| | E12.5 | 0.72 ± 0.18 | 0.80 ± 0.29 | 0.99 ± 0.29 | 0.3651 |
| | E14.5 | 0.50 ± 0.12 | 0.56 ± 0.23 | 0.63 ± 0.26 | 0.6987 |
| KYN : TRP[a] | E10.5 | 0.15 ± 0.04 | 0.15 ± 0.04 | 0.16 ± 0.04 | 0.8730 |
| | E12.5 | 0.26 ± 0.04 | 0.33 ± 0.04 | 0.25 ± 0.05 | 0.1102 |
| | E14.5 | 0.31 ± 0.03 | 0.42 ± 0.07 | 0.42 ± 0.08 | 0.1266 |

Metabolite concentrations are normalised to wet weight measured at dissection. TRP = L-tryptophan; KYN = L-kynurenine; 3HK = 3-hydroxykynurenine; 3HAA = 3-hydroxyanthranilic acid; NAMN = nicotinic acid mononucleotide; NAD+ = nicotinamide adenine dinucleotide; NAM = nicotinamide; NMN = nicotinamide mononucleotide; 2PY = N-methyl-2-pyridone-5-carboxamide; 4PY = N-methyl-4-pyridone-5-carboxamide; KA = kynurenic acid. Number of biological replicates is n = 3 for *Haao*$^{+/+}$ and *Haao*$^{+/-}$, n = 5 for *Haao*$^{-/-}$. Data is shown as mean ± standard deviation. <LOD = below the detection limit (signal:noise <3). n.a. = not applicable (significance cannot be calculated).

[a]KYN:TRP ratio was calculated for individual samples, then summarised.

[b]Statistical significance was calculated by one-way ANOVA comparing the three *Haao* genotypes, with $p<0.05$ highlighted in bold.

## Table S3.

**NAD metabolite concentrations in the visceral yolk sac at E10.5, E12.5 and E14.5 by *Haao* genotype, as measured by UHPLC-MS/MS.**

| Location | Malformation | Embryonic genotype | |
|---|---|---|---|
| | | *Haao*-/- | *Haao*+/- |
| Heart | *Total*[a] | 8/30 (27.7%) | 1/20 (5%) |
| | BAV | 5/30 (16.7%) | - |
| | VSD | 1/30 (3.3%) | - |
| | mVSD | - | 1/20 (5%) |
| | Other structural abnormalities[b] | 3/30 (10%) | - |
| Vertebrae and ribs[c] | *Total* | 19/30 (63.3%) | 0/20 (0%) |
| | Cervical vertebrae | 7/30 (23.3%) | - |
| | Thoracic vertebrae | 8/30 (26.7%) | - |
| | Lumbar vertebrae | 7/30 (23.3%) | - |
| | Sacral vertebrae | 6/30 (20%) | - |
| | Sternum | 4/30 (13.3%) | - |
| | Underdeveloped / missing ribs | 13/30 (43.3%) | - |
| Kidneys[d] | *Total* | 25/30 (83.3%) | 0/20 (0%) |
| | Hypoplasia / agenesis | 25/30 (83.3%) | - |
| | Dysmorphic | 1/30 (3.3%) | - |
| Tail | *Total* | 22/30 (73.3%) | 0/20 (0%) |
| | Caudal agenesis | 22/30 (73.3%) | - |
| Digits and Limbs | *Total* | 12/30 (40%) | 0/20 (0%) |
| | Preaxial polydactyly | 7/30 (23.3%) | - |
| | Digit-like thumb | 3/30 (10%) | - |
| | Syndactyly | 3/30 (10%) | - |
| | Talipes | 1/30 (3.3%) | - |
| Eyes | *Total* | 8/30 (26.7%) | 0/20 (0%) |
| | Microphthalmia | 8/30 (26.7%) | - |
| Abdominal wall | *Total* | 1/30 (3.3%) | 0/20 (0%) |
| | Omphalocele | 1/30 (3.3%) | - |

BAV = Bicuspid aortic valve; VSD = ventricular septal defect; mVSD = muscular ventricular septal defect.
[a]Total refers to total number of embryos having a malformation in the indicated location. Note that embryos may have multiple malformation types in each location.
[b]Other structural abnormalities refers to compact myocardium in the right ventricle (observed in two embryos) and deflated atria (observed in one embryo).
[c]Vertebral defects were included or discounted using previously established criteria (Cuny et al., 2020). Observed and counted defects include vertebral fusions, butterfly vertebrae, and hemivertebrae. Sternum defects include reduced ossification of sternebrae and asymmetrical fusion of ribs to the sternum.
[d]Kidney defects were classified as described previously (Cuny et al., 2020). In brief, kidneys with a length (tip to tip) of ≤ 1.5 mm in length were counted as hypoplastic, because the average length of a normal kidney at E18.5 is 2.98 mm (2.75-3.375 mm). The kidney classified as dysmorphic had a cyst.

## Table S4.

**Summary of congenital malformation types and incidence in embryos at E18.5 arising from maternal NW3.5 diet provision between E7.5 and E10.5.**

| Metabolite | Tissue | NW15 | | | NW3.5 | | | |
|---|---|---|---|---|---|---|---|---|
| | | *Haao+/-* | *Haao−/−* | $p^a$ | *Haao+/−* | *Haao−/−* | $p^b$ | $p^c$ |
| TRP (nmol/mg) | Embryo | 2.52 ± 0.56 | 2.75 ± 0.88 | 0.9357 | 2.19 ± 0.88 | 2.04 ± 0.81 | 0.9839 | 0.2923 |
| | Yolk sac | 2.90 ± 0.34 | 2.67 ± 0.30 | 0.4108 | 2.25 ± 0.14 | 2.38 ± 0.17 | 0.7999 | **0.0010** |
| | Ratio | 0.90 ± 0.22 | 1.05 ± 0.30 | | 0.99 ± 0.42 | 0.86 ± 0.35 | | |
| KYN (nmol/g) | Embryo | 292 ± 71.7 | 317 ± 93.9 | 0.9657 | 245 ± 136 | 225 ± 117 | 0.9826 | 0.3170 |
| | Yolk sac | 355 ± 83.1 | 337 ± 77.4 | 0.9593 | 263 ± 46.4 | 250 ± 30.8 | 0.9848 | **0.0194** |
| | Ratio | 0.88 ± 0.23 | 1.02 ± 0.33 | | 0.92 ± 0.46 | 0.89 ± 0.41 | | |
| 3HK (nmol/g) | Embryo | 13.4 ± 5.2 | 13.3 ± 4.4 | >0.9999 | 11.9 ± 6.8 | 10.4 ± 5.9 | 0.9537 | 0.6762 |
| | Yolk sac | 19.6 ± 4.3 | 30.2 ± 9.2 | 0.0299 | 13.2 ± 3.4 | 21.9 ± 5.5 | 0.0864 | **0.0009** |
| | Ratio | 0.68 ± 0.20 | 0.44 ± 0.09 | | 0.92 ± 0.53 | 0.51 ± 0.24 | | |
| 3HAA (nmol/g) | Embryo | 34.3 ± 10.1 | 434 ± 109 | <0.0001 | 22.8 ± 13.8 | 297 ± 144 | **<0.0001** | **<0.0001** |
| | Yolk sac | 42.3 ± 8.4 | 222 ± 25.5 | <0.0001 | 21.9 ± 5.2 | 179 ± 23.4 | **<0.0001** | **<0.0001** |
| | Ratio | 0.82 ± 0.16 | 1.97 ± 0.50 | | 1.04 ± 0.60 | 1.68 ± 0.75 | | |
| QA (nmol/g) | Embryo | 164 ± 98.3 | <LOD | n.a. | 170 ± 79.0 | <LOD | n.a. | n.a. |
| | Yolk sac | 225 ± 33.1 | <LOD | n.a. | 153 ± 32.9 | <LOD | n.a. | n.a. |
| | Ratio | 0.75 ± 0.40 | n.a. | | 1.06 ± 0.47 | n.a. | | |
| NAMN (nmol/g) | Embryo | 0.100 ± 0.302 | <LOD | n.a. | 0.078 ± 0.019 | 0.066 ± 0.017 | 0.7229 | 0.0704 |
| | Yolk sac | 2.14 ± 0.33 | <LOD | n.a. | 1.24 ± 0.23 | <LOD | n.a. | n.a. |
| | Ratio | 0.05 ± 0.02 | n.a. | | 0.06 ± 0.03 | n.a. | | |
| NAAD (nmol/g) | Embryo | 1.99 ± 1.42 | 0.085 ± 0.040 | 0.0006 | 0.847 ± 0.741 | 0.032 ± 0.019 | 0.2912 | **0.0003** |
| | Yolk sac | 12.3 ± 5.6 | 0.334 ± 0.340 | <0.0001 | 5.94 ± 1.07 | 0.100 ± 0.115 | **0.0420** | **<0.0001** |
| | Ratio | 0.18 ± 0.12 | 0.46 ± 0.36 | | 0.15 ± 0.14 | 1.13 ± 1.32 | | |
| NAD+ (nmol/mg) | Embryo | 4.73 ± 1.42 | 3.22 ± 0.85 | 0.0121 | 2.57 ± 0.62 | 1.12 ± 0.33 | **0.0164** | **<0.0001** |
| | Yolk sac | 4.97 ± 0.57 | 3.54 ± 0.45 | <0.0001 | 4.44 ± 0.30 | 2.42 ± 0.41 | **<0.0001** | **<0.0001** |
| | Ratio | 0.98 ± 0.34 | 0.92 ± 0.31 | | 0.58 ± 0.12 | 0.47 ± 0.19 | | |
| NAM (nmol/g) | Embryo | 145 ± 40.2 | 89.8 ± 17.1 | 0.0016 | 105 ± 30.0 | 55.0 ± 8.5 | **0.0047** | **<0.0001** |
| | Yolk sac | 605 ± 129 | 465 ± 54.9 | 0.0265 | 519 ± 35.0 | 359 ± 60.8 | **0.0103** | **0.0002** |
| | Ratio | 0.24 ± 0.07 | 0.20 ± 0.04 | | 0.20 ± 0.05 | 0.16 ± 0.03 | | |
| NMN (nmol/g) | Embryo | 13.3 ± 3.5 | 9.30 ± 2.04 | 0.0115 | 12.2 ± 1.6 | 8.56 ± 1.93 | **0.0221** | **0.0009** |
| | Yolk sac | 23.1 ± 5.8 | 13.2 ± 2.2 | 0.0022 | 14.9 ± 4.9 | 9.42 ± 1.97 | 0.1298 | **<0.0001** |
| | Ratio | 0.64 ± 0.26 | 0.70 ± 0.22 | | 0.88 ± 0.28 | 0.93 ± 0.27 | | |
| 2PY (nmol/g) | Embryo | 1.33 ± 0.78 | 1.24 ± 0.58 | 0.9474 | 0.200 ± 0.085 | 0.218 ± 0.114 | >0.9999 | **<0.0001** |
| | Yolk sac | <LOD | <LOD | n.d. | <LOD | <LOD | n.a. | n.a. |
| | Ratio | n.a. | n.a. | | n.a. | n.a. | | |
| 4PY (nmol/g) | Embryo | 1.31 ± 0.78 | 1.46 ± 0.76 | 0.9474 | 0.192 ± 0.091 | 0.185 ± 0.092 | >0.9999 | **<0.0001** |
| | Yolk sac | <LOD | <LOD | n.d. | <LOD | <LOD | n.d. | n.d. |
| | Ratio | n.a. | n.a. | | n.a. | n.a. | | |
| KA (nmol/g) | Embryo | 1.68 ± 0.53 | 1.70 ± 0.48 | 0.9998 | 1.58 ± 0.55 | 1.45 ± 0.45 | 0.9552 | 0.7401 |
| | Yolk sac | 2.40 ± 0.53 | 2.55 ± 0.52 | 0.9355 | 2.06 ± 0.29 | 1.97 ± 0.43 | 0.9864 | 0.2504 |
| | Ratio | 0.70 ± 0.23 | 0.68 ± 0.18 | | 0.80 ± 0.33 | 0.77 ± 0.20 | | |

Metabolite concentrations are normalised to total protein content in the solid fraction after metabolite extraction (tissue pellet). TRP = L-tryptophan; KYN = L-kynurenine; 3HK = 3-hydroxykynurenine; 3HAA = 3-hydroxyanthranilic acid; QA = quinolinic acid; NAMN = nicotinic acid mononucleotide; NAAD = nicotinic acid adenine dinucleotide; NAD+ = nicotinamide adenine dinucleotide; NAM = nicotinamide; NMN = nicotinamide mononucleotide; 2PY = N-methyl-2-pyridone-5-carboxamide; 4PY = N-methyl-4-pyridone-5-carboxamide; KA = kynurenic acid. n = 6 for yolk sacs, n = 8 for embryos per *Haao* genotype per condition; data shown as mean ± standard deviation. <LOD = below the detection limit (signal:noise <3). n.a. = not applicable (ratio or significance cannot be calculated).

[a,b]Statistical significance was calculated by one-way ANOVA with Tukey's multiple comparisons test comparing the two *Haao* genotypes and two dietary treatments, with the *p* values of comparing *Haao*$^{+/-}$ and *Haao*$^{-/-}$ on NW15 (a) and *Haao*$^{+/-}$ and *Haao*$^{-/-}$ on NW3.5 (b) shown and $p<0.05$ highlighted in bold.

[c]Statistical significance was calculated by one-way ANOVA comparing all four groups.

## Table S5.

**NAD metabolite concentrations in the E10.5 embryo and yolk sac with maternal NW15 or NW3.5 diet provision, normalised by protein.**

| Metabolite | Tissue | NW15 | | | NW3.5 | | | |
|---|---|---|---|---|---|---|---|---|
| | | *Haao+/-* | *Haao−/−* | *P* [a] | *Haao+/−* | *Haao−/−* | *p*[b] | *p*[c] |
| TRP (nmol/g) | Embryo | 65.8 ± 13.1 | 72.7 ± 23.4 | 0.9167 | 61.5 ± 25.2 | 57.6 ± 21.8 | 0.9825 | 0.5388 |
| | Yolk sac | 118 ± 14.3 | 118 ± 11.8 | 0.9997 | 108 ± 5.4 | 114 ± 7.3 | 0.6940 | 0.2772 |
| | Ratio | 0.57 ± 0.13 | 0.62 ± 0.18 | | 0.57 ± 0.24 | 0.52 ± 0.21 | | |
| KYN (nmol/g) | Embryo | 7.55 ± 1.48 | 8.33 ± 2.37 | 0.9430 | 6.77 ± 3.65 | 6.28 ± 3.11 | 0.9851 | 0.4833 |
| | Yolk sac | 14.3 ± 2.4 | 15.1 ± 3.9 | 0.9610 | 12.7 ± 2.6 | 12.1 ± 1.7 | 0.9794 | 0.1914 |
| | Ratio | 0.56 ± 0.11 | 0.60 ± 0.19 | | 0.52 ± 0.24 | 0.54 ± 0.23 | | |
| 3HK (nmol/g) | Embryo | 0.345 ± 0.120 | 0.353 ± 0.118 | 0.9996 | 0.329 ± 0.182 | 0.290 ± 0.158 | 0.9525 | 0.8353 |
| | Yolk sac | 0.793 ± 0.133 | 1.363 ± 0.472 | 0.0198 | 0.638 ± 0.188 | 1.067 ± 0.309 | 0.1024 | **0.0029** |
| | Ratio | 0.43 ± 0.12 | 0.26 ± 0.06 | | 0.52 ± 0.29 | 0.31 ± 0.14 | | |
| 3HAA (nmol/g) | Embryo | 0.907 ± 0.293 | 11.49 ± 3.18 | <0.0001 | 0.628 ± 0.364 | 8.30 ± 3.79 | **<0.0001** | **<0.0001** |
| | Yolk sac | 1.72 ± 0.33 | 9.95 ± 1.51 | <0.0001 | 1.06 ± 0.30 | 8.68 ± 1.48 | **<0.0001** | **<0.0001** |
| | Ratio | 0.52 ± 0.11 | 1.17 ± 0.30 | | 0.58 ± 0.32 | 1.02 ± 0.43 | | |
| QA (nmol/g) | Embryo | 4.19 ± 2.40 | <LOD | n.a. | 4.72 ± 2.12 | <LOD | n.a. | n.a. |
| | Yolk sac | 9.12 ± 0.99 | <LOD | n.a. | 7.43 ± 1.83 | <LOD | n.a. | n.a. |
| | Ratio | 0.47 ± 0.26 | n.a. | | 0.60 ± 0.25 | n.a. | | |
| NAMN (pmol/g) | Embryo | 2.63 ± 0.87 | <LOD | n.a. | 2.14 ± 0.49 | 1.93 ± 0.57 | 0.8607 | 0.1844 |
| | Yolk sac | 87.3 ± 11.9 | <LOD | n.a. | 59.62 ± 12.40 | <LOD | n.a. | n.a. |
| | Ratio | 0.60 ± 0.39 | n.a. | | 0.37 ± 0.30 | n.a. | | |
| NAAD (pmol/g) | Embryo | 50.9 ± 35.0 | 2.26 ± 1.09 | 0.0005 | 23.3 ± 20.2 | 0.910 ± 0.597 | 0.2217 | **0.0002** |
| | Yolk sac | 491 ± 187 | 15.5 ± 16.0 | <0.0001 | 286 ± 56.2 | 4.89 ± 5.78 | **0.0038** | **<0.0001** |
| | Ratio | 0.11 ± 0.07 | 0.28 ± 0.23 | | 0.08 ± 0.08 | 0.68 ± 0.80 | | |
| NAD+ (nmol/g) | Embryo | 122.3 ± 31.1 | 85.6 ± 25.9 | 0.0143 | 72.0 ± 16.7 | 31.9 ± 10.1 | **0.0069** | **<0.0001** |
| | Yolk sac | 203 ± 19.5 | 158 ± 17.2 | 0.0003 | 213 ± 10.3 | 116 ± 11.3 | **<0.0001** | **<0.0001** |
| | Ratio | 0.62 ± 0.20 | 0.54 ± 0.18 | | 0.33 ± 0.07 | 0.28 ± 0.10 | | |
| NAM (nmol/g) | Embryo | 3.80 ± 0.98 | 2.38 ± 0.55 | 0.0024 | 2.94 ± 0.81 | 1.57 ± 0.30 | **0.0032** | **<0.0001** |
| | Yolk sac | 24.6 ± 5.2 | 20.8 ± 3.1 | 0.3310 | 25.0 ± 2.1 | 17.4 ± 4.2 | **0.0144** | **0.0085** |
| | Ratio | 0.15 ± 0.04 | 0.12 ± 0.03 | | 0.12 ± 0.03 | 0.10 ± 0.02 | | |
| NMN (nmol/g) | Embryo | 0.350 ± 0.094 | 0.246 ± 0.062 | 0.0456 | 0.346 ± 0.069 | 0.246 ± 0.069 | 0.0543 | **0.0068** |
| | Yolk sac | 0.937 ± 0.210 | 0.592 ± 0.118 | 0.0165 | 0.717 ± 0.240 | 0.456 ± 0.119 | 0.0900 | **0.0013** |
| | Ratio | 0.41 ± 0.16 | 0.42 ± 0.15 | | 0.52 ± 0.21 | 0.56 ± 0.17 | | |
| 2PY (pmol/g) | Embryo | 34.0 ± 18.9 | 33.4 ± 17.5 | 0.9997 | 5.67 ± 2.44 | 6.26 ± 3.35 | 0.9997 | **<0.0001** |
| | Yolk sac | <LOD | <LOD | n.a. | <LOD | <LOD | n.a. | n.a. |
| | Ratio | n.a. | n.a. | | n.a. | n.a. | | |
| 4PY (pmol/g) | Embryo | 33.7 ± 18.9 | 39.3 ± 22.7 | 0.8738 | 5.44 ± 2.64 | 5.30 ± 2.64 | >0.9999 | **<0.0001** |
| | Yolk sac | <LOD | <LOD | n.a. | <LOD | <LOD | n.a. | n.a. |
| | Ratio | n.a. | n.a. | | n.a. | n.a. | | |
| KA (pmol/g) | Embryo | 43.3 ± 11.8 | 44.7 ± 12.3 | 0.9960 | 43.9 ± 14.5 | 40.7 ± 11.4 | 0.9560 | 0.9278 |
| | Yolk sac | 97.3 ± 19.5 | 115 ± 27.6 | 0.5470 | 98.9 ± 14.6 | 95.5 ± 24.6 | 0.9936 | 0.4428 |
| | Ratio | 0.44 ± 0.14 | 0.40 ± 0.10 | | 0.45 ± 0.16 | 0.47 ± 0.13 | | |

Metabolite concentrations are normalised to wet weight measured at dissection. TRP = L-tryptophan; KYN = L-kynurenine; 3HK = 3-hydroxykynurenine; 3HAA = 3-hydroxyanthranilic acid; QA = quinolinic acid; NAMN = nicotinic acid mononucleotide, NAAD = nicotinic acid adenine dinucleotide; NAD+, nicotinamide adenine dinucleotide; NAM = nicotinamide; NMN = nicotinamide mononucleotide; 2PY = N-methyl-2-pyridone-5-carboxamide; 4PY = N-methyl-4-pyridone-5-carboxamide; KA = kynurenic acid. n = 6 for yolk sacs, n = 8 for embryos per *Haao* genotype per condition; data shown as mean ± standard deviation. <LOD = below the detection limit (signal:noise <3). n.a. = not applicable (ratio or significance cannot be calculated).

[a,b]Statistical significance was calculated by one-way ANOVA with Tukey's multiple comparisons test comparing the two *Haao* genotypes and two dietary treatments, with the *p* values of comparing *Haao*+/- and *Haao*$^{-/-}$ on NW15 (a) and *Haao*$^{+/-}$ and *Haao*$^{-/-}$ on NW3.5 (b) shown and $p<0.05$ highlighted in bold.

[c]Statistical significance was calculated by one-way ANOVA comparing all four groups.

## Table S6.

**NAD metabolite concentrations in the E10.5 embryo and yolk sac with maternal NW15 or NW3.5 diet provision, normalised by wet weight.**

## Table S7.

**Primers for RT-qPCR.**

| Gene Symbol | Forward primer (5'-3') | Reverse primer (5'-3') |
|---|---|---|
| *Tdo2* | AGGTGCTGCTCTGCTTGTTT | TGAGCGTGTCAATGTCCATAA |
| *Ido2* | TGCCCTCAGACTTCCTCACT | CGCTGCTCACGGTAACTCTT |
| *Afmid* | AGCCACCTCCCAGAATGAC | TGGAACCACATCCAAGTGTC |
| *Kmo* | GAGCATTAACTTGGCCCTTTC | AGTGGATCATTCTGGCTTTCA |
| *Kynu* | GTTCAGTGGGCTGCACTTTT | CCCAGTCATGTAAGCGGAGT |
| *Haao* | ACAATGGGAGGGCAGTGTAT | CTTCTTACGGGCAGGGTCTT |
| *Qprt* | ACTGGTGGAGAAGTATGGGC | GGCTGCTACATTCCACCTCT |
| *Nadsyn1* | GCCAAAGGCAAAGGTGCAAG | TAGCGAACATTCCGGTGCAT |
| *Nmnat1* | GTGCCCAACTTGTGGAAGAT | CAGCACATCGGACTCGTAGA |
| *Nmnat3* | CCAGAGACCACCTACACCAAA | CCACCCGAATCCAGTCAG |
| *Ubc*[a] | CCCAGTGTTACCACCAAG | ATCACACCCAAGAACAAGC |
| *Ywhaz*[b] | CAGTAGATGGAGAAAGATTTGC | GGGACAATTAGGGAAGTAAGT |

[a]Previously published in Gu et al. (Gu et al., 2014). [b]Previously published in Jeong et al. (Jeong et al., 2014).

## Table S8.

**Summary of published RNA-seq datasets used and assessed in this study.**

| Tissue | Species | Stage | Paper | Data type; url/ accession ID; subsetting |
|---|---|---|---|---|
| Liver | Mouse | E9.5-17.5 | (Mu et al., 2020) | scRNA-seq; https://db.cngb.org/search/project/CNP0000236/ ; Subsetted out liver primordium, liver bud and hepatocytes |
| Placenta | Mouse | E9.5, E10.5, E12.5, E14.5 | (Marsh & Blelloch, 2020) | scRNA-seq; https://figshare.com/projects/Single_nuclei_RNA-seq_of_mouse_placental_labyrinth_development/92354 |
| Yolk sac | Mouse | E9.5, E10.5 | (Zhao & Choi, 2019) | scRNA-seq; https://www.ncbi.nlm.nih.gov/geo/query/acc.cgi?acc=GSM3732840 |
| Gastrulation atlas | Mouse | E6.5-8.5 | (Pijuan-Sala et al., 2019) | scRNA-seq; https://bioconductor.org/packages/devel/data/experiment/vignettes/MouseGastrulationData/inst/doc/MouseGastrulationData.html ; Subsetted two datasets for each of the following time points E8.5 (4483 cells; 7569 cells), E8.25 (4646 cells; 6707 cells) |
| Yolk sac | Human | ? | (Cindrova-Davies et al., 2017) | Bulk RNA-Seq; PRJEB18767 |
| Yolk sac | Human | 3-8 PCW | (Goh et al., 2023) | scRNA-Seq; https://app.cellatlas.io/yolk-sac/dataset/2/scatterplot ; Subsetted yolk sac endoderm |
| Liver | Human | Embryonic and adult | (Wesley et al., 2022) | scRNA-Seq; https://app.cellatlas.io/liver-development/dataset/7/scatterplot |
| Organogenesis atlas | Mouse | E10.5 | (Cao et al., 2019) | scRNA-seq; https://oncoscape.v3.sttrcancer.org/atlas.gs.washington.edu.mouse.rna/downloads ; Subsetted E10.5 only |

## Acknowledgements

This research is supported by funds to SLD from: the National Health and Medical Research Council (NHMRC), Principal Research Fellowship (ID1135886), Leadership Level 3 Fellowship (ID2007896) and Project Grant (ID1162878); a NSW Health Cardiovascular Research Capacity Program Senior Researcher Grant; and philanthropic support from the Key Foundation. We gratefully acknowledge the Victor Chang Cardiac Research Institute Innovation Centre, funded by the NSW Government, as well as funding from the Freedman Foundation for the Metabolomics Facility. We thank Joelene Greasby for technical assistance.

# References


1. Allegri G., Zaccarin D., Ragazzi E., Froldi G., Bertazzo A., Costa C. V 2003) **Metabolism of tryptophan along the kynurenine pathway in alloxan diabetic rabbits** *Adv Exp Med Biol* **527**:387–393 https://doi.org/10.1007/978-1-4615-0135-0_45

2. Alwan S., Chambers C. D 2015) **Identifying Human Teratogens: An Update** *J Pediatr Genet* **4**:39–41 https://doi.org/10.1055/s-0035-1556745

3. Bachmanov A. A., Reed D. R., Beauchamp G. K., Tordoff M. G 2002) **Food intake, water intake, and drinking spout side preference of 28 mouse strains** *Behav Genet* **32**:435–443 https://doi.org/10.1023/a:1020884312053

4. Bolger A. M., Lohse M., Usadel B 2014) **Trimmomatic: a flexible trimmer for Illumina sequence data** *Bioinformatics* **30**:2114–2120 https://doi.org/10.1093/bioinformatics/btu170

5. Brent R. L., Fawcett L. B 1998) **Nutritional studies of the embryo during early organogenesis with normal embryos and embryos exhibiting yolk sac dysfunction** *The Journal of Pediatrics* **132**:S6–S16 https://doi.org/10.1016/S0022-3476(98)70522-0

6. Brent R. L., Johnson A. J., Jensen M 1971) **The production of congenital malformations using tissue antisera** *VII. Yolk-sac antiserum. Teratology* **4**:255–275 https://doi.org/10.1002/tera.1420040302

7. Broekhuizen M., Danser A. H. J., Reiss I. K. M., Merkus D 2021) **The Function of the Kynurenine Pathway in the Placenta: A Novel Pharmacotherapeutic Target?** *Int J Environ Res Public Health* **18** https://doi.org/10.3390/ijerph182111545

8. Burke Z. D., Reed K. R., Yeh S. W., Meniel V., Sansom O. J., Clarke A. R., Tosh D 2018) **Spatiotemporal regulation of liver development by the Wnt/β-catenin pathway** *Sci Rep* **8** https://doi.org/10.1038/s41598-018-20888-y

9. Burton G. J., Fowden A. L., Thornburg K. L 2016) **Placental Origins of Chronic Disease** *Physiol Rev* **96**:1509–1565 https://doi.org/10.1152/physrev.00029.2015

10. Butler A., Hoffman P., Smibert P., Papalexi E., Satija R 2018) **Integrating single-cell transcriptomic data across different conditions, technologies, and species** *Nat Biotechnol* **36**:411–420 https://doi.org/10.1038/nbt.4096

11. Cao J., Spielmann M., Qiu X., Huang X., Ibrahim D. M., Hill A. J., Zhang F., Mundlos S., Christiansen L., Steemers F. J., Trapnell C., Shendure J 2019) **The single-cell transcriptional landscape of mammalian organogenesis** *Nature* **566**:496–502 https://doi.org/10.1038/s41586-019-0969-x

12. Chang X. B 2010) **Molecular mechanism of ATP-dependent solute transport by multidrug resistance-associated protein 1** *Methods Mol Biol* **596**:223–249 https://doi.org/10.1007/978-1-60761-416-6_11

13. Cho F. N., Chen S. N., Tai M. H., Yang T. L 2006) **The quality and size of yolk sac in early pregnancy loss** *Aust N Z J Obstet Gynaecol* **46**:413–418 https://doi.org/10.1111/j.1479-828X.2006

.00627.x

14. Cindrova-Davies T., Jauniaux E., Elliot M. G., Gong S., Burton G. J., Charnock-Jones D. S 2017) **RNA-seq reveals conservation of function among the yolk sacs of human, mouse, and chicken** *Proceedings of the National Academy of Sciences* **114**:E4753–E4761 https://doi.org/10.1073/pnas.1702560114

15. Cuny H., Bozon K., Kirk R. B., Sheng D. Z., Bröer S., Dunwoodie S. L 2023) **Maternal heterozygosity of Slc6a19 causes metabolic perturbation and congenital NAD deficiency disorder in mice** *Dis Model Mech* **16** https://doi.org/10.1242/dmm.049647

16. Cuny H., Kristianto E., Hodson M. P., Dunwoodie S. L 2021) **Simultaneous quantification of 26 NAD-related metabolites in plasma, blood, and liver tissue using UHPLC-MS/MS** *Anal Biochem* **633** https://doi.org/10.1016/j.ab.2021.114409

17. Cuny H., Rapadas M., Gereis J., Martin E., Kirk R. B., Shi H., Dunwoodie S. L 2020) **NAD deficiency due to environmental factors or gene-environment interactions causes congenital malformations and miscarriage in mice** *Proc Natl Acad Sci U S A* **117**:3738–3747 https://doi.org/10.1073/pnas.1916588117

18. Detti L., Francillon L., Christiansen M. E., Peregrin-Alvarez I., Goedecke P. J., Bursac Z., Roman R. A 2021) **Author Correction: Early pregnancy ultrasound measurements and prediction of first trimester pregnancy loss: A logistic model** *Sci Rep* **11** https://doi.org/10.1038/s41598-021-01235-0

19. Di Pietro E., Sirois J., Tremblay M. L., MacKenzie R. E. 2002) **Mitochondrial NAD-dependent methylenetetrahydrofolate dehydrogenase-methenyltetrahydrofolate cyclohydrolase is essential for embryonic development** *Mol Cell Biol* **22**:4158–4166 https://doi.org/10.1128/mcb.22.12.4158-4166.2002

20. Dobin A., Davis C. A., Schlesinger F., Drenkow J., Zaleski C., Jha S., Batut P., Chaisson M., Gingeras T. R 2013) **STAR: ultrafast universal RNA-seq aligner** *Bioinformatics* **29**:15–21 https://doi.org/10.1093/bioinformatics/bts635

21. Dong D., Reece E. A., Lin X., Wu Y., AriasVillela N., Yang P 2016) **New development of the yolk sac theory in diabetic embryopathy: molecular mechanism and link to structural birth defects** *Am J Obstet Gynecol* **214**:192–202 https://doi.org/10.1016/j.ajog.2015.09.082

22. Dunwoodie S. L., Bozon K., Szot J. O., Cuny H 2023) **Nicotinamide Adenine Dinucleotide Deficiency and Its Impact on Mammalian Development** *Antioxid Redox Signal* **39**:1108–1132 https://doi.org/10.1089/ars.2023.0349

23. Dutta A., Sinha D. K 2017) **Zebrafish lipid droplets regulate embryonic ATP homeostasis to power early development** *Open Biol* **7** https://doi.org/10.1098/rsob.170063

24. Elmore S. A., Cochran R. Z., Bolon B., Lubeck B., Mahler B., Sabio D., Ward J. M 2022) **Histology Atlas of the Developing Mouse Placenta** *Toxicol Pathol* **50**:60–117 https://doi.org/10.1177/01926233211042270

25. Gabbay-Benziv R., Reece E. A., Wang F., Yang P 2015) **Birth defects in pregestational diabetes: Defect range, glycemic threshold and pathogenesis** *World J Diabetes* **6**:481–488 https://doi.org/10.4239/wjd.v6.i3.481

26. Goh I., Botting R. A., Rose A., Webb S., Engelbert J., Gitton Y., Stephenson E., Quiroga Londoño M., Mather M., Mende N., Imaz-Rosshandler I., Yang L., Horsfall D., Basurto-Lozada D., Chipampe N. J., Rook V., Lee J. T. H., Ton M. L., Keitley D., ..., Haniffa M. 2023) **Yolk sac cell atlas reveals multiorgan functions during human early development** *Science* **381** https://doi.org/10.1126/science.add7564

27. Griffiths J., Lun A 2023) **MouseGastrulationData: Single-Cell -omics Data across Mouse Gastrulation and Early Organogenesis** *Bioconductor* https://doi.org/10.18129/B9.bioc.MouseGastrulationData

28. Gu Y., Shen X., Zhou D., Wang Z., Zhang N., Shan Z., Jin L., Lei L 2014) **Selection and Expression Profiles of Reference Genes in Mouse Preimplantation Embryos of Different Ploidies at Various Developmental Stages** *PLOS One* **9** https://doi.org/10.1371/journal.pone.0098956

29. Holliday M. A., Potter D., Jarrah A., Bearg S 1967) **The Relation of Metabolic Rate to Body Weight and Organ Size** *Pediatric Research* **1**:185–195 https://doi.org/10.1203/00006450-196705000-00005

30. Jeong J.-K., Kang M.-H., Gurunathan S., Cho S.-G., Park C., Seo H. G., Kim J.-H 2014) **Evaluation of reference genes in mouse preimplantation embryos for gene expression studies using real-time quantitative RT-PCR (RT-qPCR)** *BMC Research Notes* **7** https://doi.org/10.1186/1756-0500-7-675

31. Kaufman M. H. 1992) **The altas of mouse development** Academic Press

32. Liu J. J., Movassat J., Portha B 2019) **Emerging role for kynurenines in metabolic pathologies** *Curr Opin Clin Nutr Metab Care* **22**:82–90 https://doi.org/10.1097/mco.0000000000000529

33. Liu L., Su X., Quinn W. J., Hui S., Krukenberg K., Frederick D. W., Redpath P., Zhan L., Chellappa K., White E., Migaud M., Mitchison T. J., Baur J. A., Rabinowitz J. D. 2018) **Quantitative Analysis of NAD Synthesis-Breakdown Fluxes** *Cell Metab* **27**:1067–1080 https://doi.org/10.1016/j.cmet.2018.03.018

34. Marin M., Pătru C. L., Manolea M. M., Novac L., Dijmărescu A. L., Boldeanu M. V., Şerbănescu M. S., Boldeanu L., Iliescu D. G. 2021) **Can Ultrasound Analysis of the Yolk Sac be a Predictor of Pregnancy Outcome?** *Curr Health Sci J* **47**:547–552 https://doi.org/10.12865/chsj.47.04.10

35. Mark P., Dunwoodie S., Adam MP, Feldman J, Mirzaa GM, et al. 2023) **Congenital NAD Deficiency Disorder** *GeneReviews* Seattle: University of Washington

36. Marsh B., Blelloch R 2020) **Single nuclei RNA-seq of mouse placental labyrinth development** *eLife* **9** https://doi.org/10.7554/eLife.60266

37. Moorthie S., Blencowe H., Darlison M. W., Gibbons S., Lawn J. E., Mastroiacovo P., Morris J. K., Modell B 2018) **Chromosomal disorders: estimating baseline birth prevalence and pregnancy outcomes worldwide** *J Community Genet* **9**:377–386 https://doi.org/10.1007/s12687-017-0336-2

38. Mu T., Xu L., Zhong Y., Liu X., Zhao Z., Huang C., Lan X., Lufei C., Zhou Y., Su Y., Xu L., Jiang M., Zhou H., Lin X., Wu L., Peng S., Liu S., Brix S., Dean M., ..., Hou Y. 2020) **Embryonic liver developmental trajectory revealed by single-cell RNA sequencing in the Foxa2eGFP mouse** *Communications Biology* **3** https://doi.org/10.1038/s42003-020-01364-8

39. Notenboom R. G., Moorman A. F., Lamers W. H 1997) **Developmental appearance of ammonia-metabolizing enzymes in prenatal murine liver** *Microsc Res Tech* **39**:413–423 https://doi.org/10.1002/(sici)1097-0029(19971201)39:5<413::Aid-jemt4>3.0.Co;2-h

40. O'Rahilly R., Müller F 2010) **Developmental stages in human embryos: revised and new measurements** *Cells Tissues Organs* **192**:73–84 https://doi.org/10.1159/000289817

41. Ornoy A., Miller R. K 2023) **Yolk sac development, function and role in rodent pregnancy** *Birth Defects Res* **115**:1243–1254 https://doi.org/10.1002/bdr2.2172

42. Ouyang J. F., Kamaraj U. S., Cao E. Y., Rackham O. J. L 2021) **ShinyCell: simple and sharable visualization of single-cell gene expression data** *Bioinformatics* **37**:3374–3376 https://doi.org/10.1093/bioinformatics/btab209

43. Oxenkrug G. F 2015) **Increased Plasma Levels of Xanthurenic and Kynurenic Acids in Type 2 Diabetes** *Mol Neurobiol* **52**:805–810 https://doi.org/10.1007/s12035-015-9232-0

44. Pang Z., Zhou G., Ewald J., Chang L., Hacariz O., Basu N., Xia J 2022) **Using MetaboAnalyst 5.0 for LC–HRMS spectra processing, multi-omics integration and covariate adjustment of global metabolomics data** *Nature Protocols* **17**:1735–1761 https://doi.org/10.1038/s41596-022-00710-w

45. Perez-Garcia V., Fineberg E., Wilson R., Murray A., Mazzeo C. I., Tudor C., Sienerth A., White J. K., Tuck E., Ryder E. J., Gleeson D., Siragher E., Wardle-Jones H., Staudt N., Wali N., Collins J., Geyer S., Busch-Nentwich E. M., Galli A., ..., Hemberger M. 2018) **Placentation defects are highly prevalent in embryonic lethal mouse mutants** *Nature* **555**:463–468 https://doi.org/10.1038/nature26002

46. Pijuan-Sala B., Griffiths J. A., Guibentif C., Hiscock T. W., Jawaid W., Calero-Nieto F. J., Mulas C., Ibarra-Soria X., Tyser R. C. V., Ho D. L. L., Reik W., Srinivas S., Simons B. D., Nichols J., Marioni J. C., Göttgens B 2019) **A single-cell molecular map of mouse gastrulation and early organogenesis** *Nature* **566**:490–495 https://doi.org/10.1038/s41586-019-0933-9

47. Reece E. A., Pinter E., Homko C., Wu Y. K., Naftolin F 1994) **The yolk sac theory: closing the circle on why diabetes-associated malformations occur** *J Soc Gynecol Investig* **1**:3–13

48. Ross C., Boroviak T. E 2020) **Origin and function of the yolk sac in primate embryogenesis** *Nat Commun* **11** https://doi.org/10.1038/s41467-020-17575-w

49. Sedlmayr P., Blaschitz A., Stocker R 2014) **The role of placental tryptophan catabolism** *Front Immunol* **5** https://doi.org/10.3389/fimmu.2014.00230

50. Seifert J 2017) **Embryo yolk sac membrane kynurenine formamidase of l-tryptophan to NAD(+) pathway as a primary target for organophosphorus insecticides (OPI) in OPI-induced NAD-associated avian teratogenesis** *Toxicol In Vitro* **44**:357–360 https://doi.org/10.1016/j.tiv.2017.08.001

51. Seifert J., Casida J. E 1978) **Relation of yolk sac membrane kynurenine formamidase inhibition to certain teratogenic effects of organophosphorus insecticides and of carbaryl and eserine in chicken embryos** *Biochem Pharmacol* **27**:2611–2615 https://doi.org/10.1016/0006-2952(78)90335-0

52. Seifert J., Casida J. E 1979) **Inhibition and reactivation of chicken kynurenine formamidase: In vitro studies with organophosphates, N-alkylcarbamates, and phenylmethanesulfonyl**

**fluoride** *Pesticide Biochemistry and Physiology* **12**:273–279 https://doi.org/10.1016/0048-3575(79)90112-3

53. Shi H., Enriquez A., Rapadas M., Martin E., Wang R., Moreau J., Lim C. K., Szot J. O., Ip E., Hughes J. N., Sugimoto K., Humphreys D. T., McInerney-Leo A. M., Leo P. J., Maghzal G. J., Halliday J., Smith J., Colley A., Mark P. R., ..., Dunwoodie S. L. 2017) **NAD Deficiency, Congenital Malformations, and Niacin Supplementation** *N Engl J Med* **377**:544–552 https://doi.org/10.1056/NEJMoa1616361

54. Spinelli P., Latchney S. E., Reed J. M., Fields A., Baier B. S., Lu X., McCall M. N., Murphy S. P., Mak W., Susiarjo M 2018) **Identification of the novel Ido1 imprinted locus and its potential epigenetic role in pregnancy loss** *Human Molecular Genetics* **28**:662–674 https://doi.org/10.1093/hmg/ddy383

55. Suguna B., Sukanya K 2019) **Yolk sac size & shape as predictors of first trimester pregnancy outcome: A prospective observational study** *J Gynecol Obstet Hum Reprod* **48**:159–164 https://doi.org/10.1016/j.jogoh.2018.10.016

56. Szot J. O., Campagnolo C., Cao Y., Iyer K. R., Cuny H., Drysdale T., Flores-Daboub J. A., Bi W., Westerfield L., Liu P., Leung T. N., Choy K. W., Chapman G., Xiao R., Siu V. M., Dunwoodie S. L 2020) **Bi-allelic Mutations in NADSYN1 Cause Multiple Organ Defects and Expand the Genotypic Spectrum of Congenital NAD Deficiency Disorders** *Am J Hum Genet* **106**:129–136 https://doi.org/10.1016/j.ajhg.2019.12.006

57. Szot J. O., Cuny H., Martin E. M., Sheng D. Z., Iyer K., Portelli S., Nguyen V., Gereis J. M., Alankarage D., Chitayat D., Chong K., Wentzensen I. M., Vincent-Delormé C., Lermine A., Burkitt-Wright E., Ji W., Jeffries L., Pais L. S., Tan T. Y., ..., Dunwoodie S. L. 2024) **A metabolic signature for NADSYN1-dependent congenital NAD deficiency disorder** *J Clin Invest* **134** https://doi.org/10.1172/jci174824

58. Szot J. O., Slavotinek A., Chong K., Brandau O., Nezarati M., Cueto-González A. M., Patel M. S., Devine W. P., Rego S., Acyinena A. P., Shannon P., Myles-Reid D., Blaser S., Mieghem T. V., Yavuz-Kienle H., Skladny H., Miller K., Riera M. D. T., Martínez S. A., ..., Dunwoodie S. L. 2021) **New cases that expand the genotypic and phenotypic spectrum of Congenital NAD Deficiency Disorder** *Hum Mutat* **42**:862–876 https://doi.org/10.1002/humu.24211

59. Terlouw G. D., Bechter R 1992) **Comparison of the metabolic activity of yolk sac tissue in the whole embryo and isolated yolk sac culture** *Reprod Toxicol* **6**:85–92 https://doi.org/10.1016/0890-6238(92)90025-o

60. Walsh J. L., Todd W. P., Carpenter B. K., Schwarcz R 1991) **4-halo-3-hydroxyanthranilic acids: potent competitive inhibitors of 3-hydroxy-anthranilic acid oxygenase in vitro** *Biochem Pharmacol* **42**:985–990 https://doi.org/10.1016/0006-2952(91)90279-e

61. Wang Y., Guan Y., Xie Q., Gong W., Li J., Chen T., Xu Y., Xu N., Chen S., Chen M., Wang Z., Hao C. M 2023) **The metabolites of de novo NAD(+) synthesis are a valuable predictor of acute kidney injury** *Clin Kidney J* **16**:711–721 https://doi.org/10.1093/ckj/sfac262

62. Wesley B. T., Ross A. D. B., Muraro D., Miao Z., Saxton S., Tomaz R. A., Morell C. M., Ridley K., Zacharis E. D., Petrus-Reurer S., Kraiczy J., Mahbubani K. T., Brown S., Garcia-Bernardo J., Alsinet C., Gaffney D., Horsfall D., Tysoe O. C., Botting R. A., ..., Vallier L. 2022) **Single-cell atlas of**

**human liver development reveals pathways directing hepatic cell fates** *Nat Cell Biol* **24**:1487–1498 https://doi.org/10.1038/s41556-022-00989-7

63. Xiao W., Wang R. S., Handy D. E., Loscalzo J 2018) **NAD(H) and NADP(H) Redox Couples and Cellular Energy Metabolism** *Antioxid Redox Signal* **28**:251–272 https://doi.org/10.1089/ars.2017.7216

64. Yang L., Wang W. H., Qiu W. L., Guo Z., Bi E., Xu C. R 2017) **A single-cell transcriptomic analysis reveals precise pathways and regulatory mechanisms underlying hepatoblast differentiation** *Hepatology* **66**:1387–1401 https://doi.org/10.1002/hep.29353

65. Zhao H., Choi K 2019) **Single cell transcriptome dynamics from pluripotency to FLK1(+) mesoderm** *Development* **146** https://doi.org/10.1242/dev.182097

## Author information

**Kayleigh Bozon**
Victor Chang Cardiac Research Institute, Sydney, Australia
ORCID iD: 0000-0002-2910-7616

**Hartmut Cuny**
Victor Chang Cardiac Research Institute, Sydney, Australia, School of Clinical Medicine, Faculty of Medicine and Health, University of New South Wales, Sydney, Australia
ORCID iD: 0000-0002-1551-2354

**Delicia Z Sheng**
Victor Chang Cardiac Research Institute, Sydney, Australia

**Ella MMA Martin**
Victor Chang Cardiac Research Institute, Sydney, Australia

**Alena Sipka**
Victor Chang Cardiac Research Institute, Sydney, Australia

**Paul Young**
Victor Chang Cardiac Research Institute, Sydney, Australia

**David T Humphreys**
Victor Chang Cardiac Research Institute, Sydney, Australia, School of Clinical Medicine, Faculty of Medicine and Health, University of New South Wales, Sydney, Australia
ORCID iD: 0000-0003-4140-0089

**Sally L Dunwoodie**
Victor Chang Cardiac Research Institute, Sydney, Australia, School of Clinical Medicine, Faculty of Medicine and Health, University of New South Wales, Sydney, Australia
ORCID iD: 0000-0002-2069-7349

**For correspondence:** s.dunwoodie@victorchang.edu.au

## Editors

Reviewing Editor
**Juan Pedro Martinez-Barbera**
University College London, London, United Kingdom

Senior Editor
**Wei Yan**
Washington State University, Pullman, United States of America

**Reviewer #1 (Public review):**

Summary:

This study investigated the mechanism underlying Congenital NAD Deficiency Disorder (CNDD) using a mouse model with loss of function of the HAAO enzyme which mediates a key step in the NAD de novo synthesis pathway. This study builds on the observation that the kynurenine pathway is required in the conceptus, as HOO null embryos are sensitive to maternal deficiency of NAD precursors (vitamin B3) and tryptophan, and narrows the window of sensitivity to a 3 day period.

An important finding is that de novo NAD synthesis occurs in an extra-embryonic tissue, the visceral yolk sac, before the liver develops in the embryo. It is suggested that lack of this yolk sac activity leads to impaired NAD supply in the embryo leading to structural abnormalities found later in development.

Strengths:

Previous studies show a requirement for HAOO activity for normal development of the embryos develop abnormalities under conditions of maternal vitamin B3 deficiency, indicating a requirement for NAD synthesis in the conceptus. Analysis of scRNA-seq datasets combined with metabolite analysis of yolk sac tissue shows that the NAD synthesis pathway is expressed and functional in the yolk sac from E10.5 onwards (prior to liver development).

HAOO enzyme assay enabled quantification of enzyme activity in relevant tissues including liver (from E12.5), embryo, placenta and yolk sac (from E11.5).
Comprehensive metabolite analysis of the NAD synthesis pathway supports the predicted effects of HAOO knockout and provides analysis of yolk sac, placenta and embryo at a series of stages.

The dietary study (with lower vitamin B3 in maternal diet from E7.5-10.5) is an incremental addition to previous studies which imposed similar restrictions from E7.5-12.5. Nevertheless, this emphasises the importance of the synthesis pathway on the conceptus at stages before liver activity is prominent.

Weaknesses:

The current dietary study narrows the period when deficiency can cause malformations (analysed at E18.5), and altered metabolite profiles (eg, increased 3HAA, lower NAD) are detected in yolk sac and embryo at E10.5.

More importantly, there is still a question of whether in addition to the yolks sac, there is HAAO activity within the embryo itself has been assayed as early as E11.5, with minimal activity prior to E12.5 (when it is assayed in liver). These findings support the hypothesis that within the conceptus (embryo, chorioallantoic placenta and visceral yok sac) the embryo is unlikely to be the site of NAD synthesis prior to liver development.

Evidence for lack of function of the NAD synthesis pathway in the embryos itself from kynurenine at E7.5-10.5 comes from reanalysis of scRNA-seq. This suggests low or absent expression of HAAO in the embryo prior to E10.5 (corresponding to the period when the authors have demonstrated that de novo NAD synthesis in the conceptus is needed). The caveat to this conclusion is that additional analysis of RNA and/or protein expression in the embryos at E7.5-10.5 has not been performed to validate the scRNA-seq data.

https://doi.org/10.7554/eLife.97649.2.sa2

**Reviewer #2 (Public review):**

Summary:

Disruption of the nicotinamide adenine dinucleotide (NAD) de novo Synthesis Pathway, by which L-tryptophan is converted to NAD results in multi-organ malformations which collectively has been termed Congenital NAD Deficiency Disorder (CNDD).

While NAD de novo synthesis is primarily active in the liver postnatally, the site of activity prior to and during organogenesis is unknown. However, mouse embryos are susceptible to CNDD between E7.5-E12.5, before the embryo has developed a functional liver. Therefore, NAD de novo synthesis is likely active in another cell or tissue during this time window of susceptibility.

The body of work presented in this paper continues the corresponding author's labs investigation of the cause and effects of NAD Deficiency and the primary goal was to determine the cell or tissue responsible for NAD de novo synthesis during early embryogenesis.

The authors conclude that visceral yolk sac endoderm is the source of NAD de novo synthesis, which is essential for mouse embryonic development, and furthermore that the dynamics of NAD synthesis are conserved in human equivalent cells and tissues, the perturbation of which results in CNDD.

Strengths:

Overall, the primary findings regarding the source of NAD synthesis, the temporal requirement and conservation between rodent and human species is quite novel and important for our understanding of NAD synthesis and function and role in CNDD.

The authors used UHPLC-MS/MS to quantify NAD+ and NAD-related metabolites and showed convincingly that the NAD salvage pathway can compensate for the loss of NAD synthesis in Halo-/- embryos, then determined that Haao activity was present in the yolk sac prior to hepatic development identifying this organ as the site of de novo NAD synthesis. Dietary modulation between E7.5-10.5 was sufficient to induce CNDD phenotypes, narrowing the window of susceptibility, and then re-analysis of RNA-seq datasets suggested the endoderm was the cell source of NAD synthesis.

Weaknesses:

Page 4 and Table S4. The descriptors for malformations of organs such as the kidney and vertebrae are quite vague and uninformative. More specific details are required to convey the type and range of anomalies observed as a consequence of NAD deficiency.

Can the authors define whether the role for the NAD pathway in a couple of tissue or organ systems is the same. By this I mean is the molecular or cellular effect of NAD deficiency the same in the vertebrae and organs such as the kidney. What unifies the effects on these

specific tissues and organs and are all tissues and organs affected. If some are not, can the authors explain why they escape the need for the NAD pathway.

Page 5 and Figure 6C. The expectation and conclusion for whether specific genes are expressed in particular cell types in scRNA-seq datasets depends on number of cells sequenced, the technology (methodology) used, the depth of sequencing and also the resolution of the analysis. It is therefore essential to perform secondary validation of the analysis of scRNA-seq data. At a minimum, the authors should perform in situ hybridization or immunostaining for Tdo2, Amid, Kmo, Kanu, Haas, Qprt and Nadsyn1 or some combination thereof at multiple time points during early mouse embryogenesis to truly understand the spatiotemporal dynamics of expression and NAD synthesis.

Absolute functional proof of the yolk sac endoderm as being essential and required for NAD synthesis in the context of CNDD might require conditional deletion of Haoo in the yolk sac versus embryo using appropriate Cre driver lines or in the absence of a conditional allele, could be performed by tetraploid embryo-ES cell complementation approaches. But temporal dietary intervention can also approximate the same thing by perturbing NAD synthesis then the yolk sac is the primary source versus when the liver becomes the primary source in the embryo.

In further revisions, the authors have added data to Supp Table 4 and Supplemental Figures 1 and 2

Although the authors did not perform in situ hybridization for some of the genes requested to define the critical cell type of expression, available scRNA-sequencing suggests the endoderm and yolk sac are the only likely source of NAD synthesis prior to its synthesis in the liver. Absolute functional proof of the yolk sac endoderm as being essential and required for NAD synthesis in the context of CNDD still requires validation but nonetheless it seems likely given the absence of the liver in some embryos. The authors provided some additional data pertaining to the type of kidney and vertebral anomalies observed which makes this data more complete.

https://doi.org/10.7554/eLife.97649.2.sa1

**Author response:**

The following is the authors' response to the original reviews.

> ***Reviewer 1 Public Review:***
>
> *The current dietary study narrows the period when deficiency can cause malformations (analysed at E18.5), and altered metabolite profiles (eg, increased 3HAA, lower NAD) are detected in the yolk sac and embryo at E10.5. However, without analysis of embryos at later stages in this experiment it is not known how long is needed for NAD synthesis to be recovered - and therefore until when the period of exposure to insufficient NAD lasts. This information would inform the understanding of the developmental origin of the observed defects.*

Our previous published work (Cuny et al 2023 https://doi.org/10.1242/dmm.049647) indicates that the timing of NAD *de novo* synthesis pathway precursor availability and consequently the timing of NAD deficiency during organogenesis drives which organs are affected in their development. Furthermore, experimental data of another project (manuscript submitted) shows that mouse embryos (from mothers on an NAD precursor restricted diet that induces CNDD) were NAD deficient at E9.5 and E11.5, but embryo NAD levels were fully recovered at E14.5 when compared to same-stage embryos from mothers on precursor-sufficient diet. This

was observed irrespective of the embryos' *Haao* genotype. In the current study, NAD precursor provision was only restricted until E10.5. Thus, we expect that our embryos phenotyped at E18.5 had recovered their NAD levels back to normal by E14.5 at the latest. More research, beyond the scope of the current manuscript, is required to spatio-temporally link embryonic NAD deficiency to the occurrence of specific defect types and elucidate the mechanistic origin of the defects. To acknowledge this, we updated the respective Discussion paragraph on page 7 and added the following statement: "This observation supports our hypothesis that the timing of NAD deficiency during organogenesis determines which organs/tissues are affected (Cuny et al., 2023), but more research is needed to fully characterise the onset and duration of embryonic NAD deficiency in dietary NAD precursor restriction mouse models."

> *More importantly, there is still a question of whether in addition to the yolk sac, there is HAAO activity within the embryo itself prior to E12.5 (when it has first been assayed in the liver - Figure 1C). The prediction is that within the conceptus (embryo, chorioallantoic placenta, and visceral yok sac) the embryo is unlikely to be the site of NAD synthesis prior to liver development. Reanalysis of scRNA-seq (Fig 1B) shows expression of all the enzymes of the kynurenine pathway from E9.5 onwards. However, the expression of another available dataset at E10.5 (Fig S3) suggested that expression is 'negligible'. While the expression in Figure 1B, Figure S1 is weak this creates a lack of clarity about the possible expression of HAAO in the hepatocyte lineage, or especially elsewhere in the embryo prior to E10.5 (corresponding to the period when the authors have demonstrated that de novo NAD synthesis in the conceptus is needed). Given these questions, a direct analysis of RNA and/or protein expression in the embryos at E7.5-10.5 would be helpful.*

We now have included additional data showing that whole embryos at E11.5 and embryos with their livers removed at E14.5 have negligible HAAO enzyme activity. The observed lack of HAAO activity in the embryo at E11.5 is consistent with the absence of a functional embryonic liver at that stage. Thus, it confirms that the embryo is dependent of extraembryonic tissues (the yolk sac) for NAD *de novo* synthesis prior to E12.5. The additional datasets are now included in Supplementary Table S1 and as Supplementary Figure 2. The Results section on page 2 has been updated to refer to these datasets.

> ***Reviewer #2 (Public Review):***
>
> *Page 4 and Table S4. The descriptors for malformations of organs such as the kidney and vertebrae are quite vague and uninformative. More specific details are required to convey the type and range of anomalies observed as a consequence of NAD deficiency.*

We now provide more information about the malformation types in the Results on page 4. Also, Table S4 now defines the missing vertebral, sternum, and kidney descriptors.

> *Can the authors define whether the role of the NAD pathway in a couple of tissue or organ systems is the same? By this I mean is the molecular or cellular effect of NAD deficiency is the same in the vertebrae and organs such as the kidney. What unifies the effects on these specific tissues and organs and are all tissues and organs affected? If some are not, can the authors explain why they escape the need for the NAD pathway?*

This is a good comment, highlighting that further research, beyond the scope of this manuscript, is needed to better understand the underlying mechanisms of CNDD causation. We have expanded the Discussion paragraph "NAD deficiency in early organogenesis is sufficient to cause CNDD" to indicate that while the timing of NAD deficiency during embryogenesis explains variability in phenotypes among the CNDD spectrum, it is unknown why other organs/tissues are seemingly not affected by NAD deficiency.

To answer the reviewer's questions and elucidate the underlying cellular and molecular processes in individual organs affected by NAD deficiency, a multiomic approach is required. This is because NAD is involved in hundreds of molecular and cellular processes affecting gene expression, protein levels, metabolism, etc. For details of NAD functions that have relevance to embryogenesis, the reviewer may refer to our recent review article (Dunwoodie et al 2023 https://doi.org/10.1089/ars.2023.0349).

> *Page 5 and Figure 6C. The expectation and conclusion for whether specific genes are expressed in particular cell types in scRNA-seq datasets depend on the number of cells sequenced, the technology (methodology) used, the depth of sequencing, and also the resolution of the analysis. It is therefore essential to perform secondary validation of the analysis of scRNA-seq data. At a minimum, the authors should perform in situ hybridization or immunostaining for Tdo2, Amid, Kmo, Kanu, Haas, Qprt, and Nadsyn1 or some combination thereof at multiple time points during early mouse embryogenesis to truly understand the spatiotemporal dynamics of expression and NAD synthesis.*

We have tested antibodies against HAAO, KYNU, and QPRT in adult mouse liver samples (the main site of NAD *de novo* synthesis) but these produced non-specific bands in western blotting experiments. Therefore, immunostaining studies on embryonic tissues were not feasible.

However, we agree that histological methods such as *in situ* hybridisation would provide secondary validation of the exact cell types that express these genes. To acknowledge this, we have updated a sentence on page 5 referring to the data shown in Figure 6C as follows: "While histological methods such as *in situ* hybridisation would be required to confirm the exact cell types expressing these genes, the available expression data indicates that the genes encoding those enzymes required to convert L-kynurenine to NAD (kynurenine pathway) are exclusively expressed in the yolk sac endoderm lineage from the onset of organogenesis (E8.0-8.5)."

> *Absolute functional proof of the yolk sac endoderm as being essential and required for NAD synthesis in the context of CNDD might require conditional deletion of Haoo in the yolk sac versus embryo using appropriate Cre driver lines or in the absence of a conditional allele, could be performed by tetraploid embryo-ES cell complementation approaches. But temporal dietary intervention can also approximate the same thing by perturbing NAD synthesis Shen the yolk sac is the primary source versus when the liver becomes the primary source in the embryo.*

Reviewer 1 has made a similar comment about confirming that indeed NAD *de novo* synthesis activity is limited to extraembryonic tissues (=yolk sacs) and absent in the embryo prior to development of an embryonic liver. We now have included additional data showing that whole embryos at E11.5 and embryos with their livers removed at E14.5 have negligible HAAO enzyme activity. The observed lack of HAAO activity in the embryo at E11.5 is consistent with the absence of a functional embryonic liver at that stage. We think this provides enough proof that the embryo is dependent of extraembryonic tissues (the yolk sac) for NAD *de novo* synthesis prior to E12.5. The additional datasets are now included in Supplementary Table S1 and as Supplementary Figure 2. The Results section on page 2 has been updated to refer to these data.

> ***Reviewer #1 (Recommendations For The Authors):***
>
> *(1) Introduction (page 1) introduces mouse models with defects in the kynurenine pathway "confirming that NAD de novo synthesis is required during embryogenesis ...". This requirement is revealed by the imposition of maternal dietary deficiency and more*

> *detail (or a more clear link to the following sentences) here would help the reader who is not familiar with the previous papers using the HAAO mice and dietary modulation.*

We have updated this paragraph in the Introduction to better indicate that the requirement of NAD *de novo* synthesis for embryogenesis was confirmed in mouse models by modulating the maternal dietary NAD precursor provision during pregnancy.

> *(2) Discussion - throughout the introduction and results the authors refer to the NAD de novo synthesis pathway, with the study focussing on the effects of HAAO loss of function. Data implies that the kynurenine pathway is active in the yolk sac but whether de novo synthesis from L-tryptophan occurs has not been addressed. The first sub-heading of the discussion could be more accurate referring to the kynurenine pathway, or synthesis from kynurenine.*

We agree that our manuscript needed to make better distinction between NAD *de novo* synthesis starting from kynurenine and starting from tryptophan. We removed "from Ltryptophan" from the sub-heading in the Discussion and clarified in this paragraph which genes are required to convert tryptophan to kynurenine and which genes to convert kynurenine to NAD. We also updated two Results paragraphs (page 2, 2nd paragraph; page 5, 5th paragraph) to improve clarity.

It is worth noting that our statement in the Discussion "this is the first demonstration of NAD *de novo* synthesis occurring in a tissue outside of the liver and kidney." is valid because vascular smooth muscle cells express *Tdo2* and in combination with the other requisite genes expressed in endoderm cells, the yolk sac has the capability to synthesise NAD *de novo* from L-tryptophan.

> *(3) Outlook - While this section is designed to be looking ahead to the potential implications of the work, the last section on gene therapy of the yolk sac seems far removed from the paper content and highly speculative. I feel this could detract from the main points of the study and could be removed.*

We have updated the Outlook paragraph and shortened the final part to "Further research is required to better understand the mechanisms of CNDD causation and of other causes of adverse pregnancy outcomes involving the yolk sac."

> *(4) In Figure 2D it would be useful to label the clusters as the colours in the legend are difficult to match to the heatmap.*

We now have labelled the clusters with lowercase letters above the heatmap to make it easier to match the clusters in Figure 2D to the colours used for designating tissues and genotypes. These labels are described in the figure's key and the figure legend.

> ***Reviewer #2 (Recommendations For The Authors):***
>
> *Page 4 and Table S4. The descriptors for malformations of organs such as the kidney and vertebrae are quite vague and uninformative. More specific details are required to convey the type and range of anomalies observed as a consequence of NAD deficiency.*

We now provide more information about the malformation types in the Results on page 4. Also, Table S4 now defines the missing vertebral, sternum, and kidney descriptors.

> *Can the authors define whether the role of the NAD pathway in a couple of tissue or organ systems is the same? By this I mean is the molecular or cellular effect of NAD deficiency is the same in the vertebrae and organs such as the kidney. What unifies the*

> *effects on these specific tissues and organs and are all tissues and organs affected? If some are not, can the authors explain why they escape the need for the NAD pathway?*

This is a good comment, highlighting that further research, beyond the scope of this manuscript, is needed to better understand the underlying mechanisms of CNDD causation. We have expanded the Discussion paragraph "NAD deficiency in early organogenesis is sufficient to cause CNDD" to indicate that while the timing of NAD deficiency during embryogenesis explains variability in phenotypes among the CNDD spectrum, it is unknown why other organs/tissues are seemingly not affected by NAD deficiency.

To answer the reviewer's questions and elucidate the underlying cellular and molecular processes in individual organs affected by NAD deficiency, a multiomic approach is required. This is because NAD is involved in hundreds of molecular and cellular processes affecting gene expression, protein levels, metabolism, etc. For details of NAD functions that have relevance to embryogenesis, the reviewer may refer to our recent review article (Dunwoodie et al 2023 https://doi.org/10.1089/ars.2023.0349).

> *Page 5 and Figure 6C. The expectation and conclusion for whether specific genes are expressed in particular cell types in scRNA-seq datasets depend on the number of cells sequenced, the technology (methodology) used, the depth of sequencing, and also the resolution of the analysis. It is therefore essential to perform secondary validation of the analysis of scRNA-seq data. At a minimum, the authors should perform in situ hybridization or immunostaining for Tdo2, Amid, Kmo, Kanu, Haas, Qprt, and Nadsyn1 or some combination thereof at multiple time points during early mouse embryogenesis to truly understand the spatiotemporal dynamics of expression and NAD synthesis.*

We have tested antibodies against HAAO, KYNU, and QPRT in adult mouse liver samples (the main site of NAD *de novo* synthesis) but these produced non-specific bands in western blotting experiments. Therefore, immunostaining studies on embryonic tissues were not feasible.

However, we agree that histological methods such as *in situ* hybridisation would provide secondary validation of the exact cell types that express these genes. To acknowledge this, we have updated a sentence on page 5 referring to the data shown in Figure 6C as follows: "While histological methods such as *in situ* hybridisation would be required to confirm the exact cell types expressing these genes, the available expression data indicates that the genes encoding those enzymes required to convert L-kynurenine to NAD (kynurenine pathway) are exclusively expressed in the yolk sac endoderm lineage from the onset of organogenesis (E8.0-8.5)."

https://doi.org/10.7554/eLife.97649.2.sa0